A UNITED STATES DEPARTMENT OF COMMERCE PUBLICATION

essa

Professional Paper 4

U.S. DEPARTMENT OF COMMERCE / Environmental Science Services Administration

A SURVEY AND ANALYSIS OF Normal Ionospheric Absorption Measurements OBTAINED FROM RADIO PULSE REFLECTIONS

essa Professional Paper 4

A SURVEY AND ANALYSIS OF

Normal Ionospheric Absorption Measurements

OBTAINED FROM RADIO PULSE REFLECTIONS

LARRY D. SCHULTZ AND ROGER M. GALLET
Institute for Telecommunication Sciences
Research Laboratories, Boulder, Colorado

U.S. DEPARTMENT OF COMMERCE, Maurice H. Stans, *Secretary*
ENVIRONMENTAL SCIENCE SERVICES ADMINISTRATION, Robert M. White, *Administrator*

Rockville, Md., September 1970

UDC 551.510.535:621.391.812.63

551.510.535	Ionosphere
621.391	Electrical communications
.812	Variations in signal intensity
.63	Ionospheric absorption

For sale by the Superintendent of Documents, U.S. Government Printing Office
Washington, D.C. 20402 - Price 45 cents

Contents

LIST OF FIGURES

LIST OF TABLES

A SURVEY AND ANALYSIS OF

Normal Ionospheric Absorption Measurements

OBTAINED FROM RADIO PULSE REFLECTIONS

Larry D. Schultz and Roger M. Gallet

ABSTRACT.—An analysis of published midday absorption data obtained by the reflection method of vertical incidence sounding quantitatively establishes the existence of an equatorial absorption anomaly. This anomaly is the abnormally large variation of the amplitude of the seasonal variation observed at equatorial latitudes. It is suggested that certain D-region dynamical processes cause this anomaly. In addition, the analysis disclosed the unexpected existence of a significant latitudinal variation of absorption not due to the $\cos^n\chi$ variation; the order of magnitude of this latitudinal variation is of the same order as the variation of absorption due to the sunspot cycle. This latitudinal variation, together with the latitudinal variation of the E-layer critical frequency, indicates that the electron producing mechanisms for the lower ionosphere vary systematically with latitude and solar activity. For middle latitudes, the analysis reconfirmed results obtained previously by other authors.

The total variation of lower ionosphere absorption is separated into the four categories: (1) seasonal variation with latitudinal effects, (2) latitudinal variation, (3) solar cycle variation, and (4) winter anomaly effects. Empirically derived formulas are given which permit the calculation of each of these four variations and also the calculation of the total lower ionosphere absorption losses of HF radio waves propagating via the ionosphere both at vertical and at oblique incidence.

INTRODUCTION

In recent years, emphasis in the literature has been on the effects of abnormal ionospheric absorption (i.e., polar-cap and auroral absorption) on HF and VHF radio waves propagating in polar regions. By comparison, the effects of normal ionospheric absorption (i.e., nondeviative D-region absorption) on propagation have been somewhat neglected, even though such effects apply to a much larger area of the earth's surface. This neglect of normal D-region absorption effects on propagation seems due to the widespread belief that all absorption effects are well known and well understood, and that little would be gained by additional study in this field. Such a belief exists because different independent analyses of absorption data obtained at middle latitudes by several ionosphere physicists (Rawer 1949 and 1952; Piggott 1953; Appleton and Piggott 1954) have all yielded results which are in good agreement with each other and with results predicted by classical photoionization theory (Appleton 1937; Nicolet and Bossy 1949; Mitra and Jain 1963).

The usual procedure has been to apply the classical theory of photoionization to equatorial regions, because photoionization processes are assumed to be predominant at equatorial regions and observations at middle latitudes support results predicted by the theory. This procedure is not correct, however, since results predicted by the theory disagree

with equatorial observations. The reason for the disagreement is that the classical theory of photoionization incorrectly assumes that the D region is formed by uniform photoionization processes and that there are no systematic changes with latitude in the structure of the D region.

An early indication that lower ionosphere processes vary with latitude was the finding of a systematic latitudinal variation of the E-layer critical frequency f_E in addition to the usual variation caused by the solar zenith angle. This variation is given by (Harnischmacher 1950)

$$f_E = K \cos^n \chi,$$

where

$$K = 2.25 + 1.5 \cos \lambda + [0.01 - 0.007 \cos \lambda] R_{13}$$

and

$$n = 0.21 + 0.12 \cos \lambda + 0.002 R_{13}.$$

The quantity χ is the solar zenith angle, λ is the geographic latitude, and R_{13} is the 13-month running average of the mean monthly sunspot number.

Another indication that D-region absorption processes were not the same for all latitudes was first reported by one of the present authors (Delobeau and Gallet 1954). At that time, it was pointed out that the amplitude of the seasonal variation of absorption at equatorial latitudes was very large when compared with results found at middle latitudes and also with results predicted by classical photoionization theory. It was suggested that this anomalous behavior be examined further when more equatorial absorption data became available. To the best of the present authors' knowledge, such an analysis has not yet been given in the literature.

More recent evidence that D-region formation processes and, therefore, absorption effects vary with latitude has come from the study of galactic cosmic rays and their influence on the ionosphere. These phenomena produce large amounts of electrons (up to several hundred electrons/cm^3) at D-region heights in high geomagnetic latitudes. Cosmic rays do not appear to have a diurnal variation but they are inversely correlated with solar activity (during sunspot maximum the sun ejects more plasmas containing magnetic fields which tend to repel cosmic ray particles entering the solar system). The effects of these two phenomena are beyond the scope of this paper, and therefore their effects are not discussed or included in this analysis.

The authors became interested in the calculation of lower ionosphere absorption measurements through the problem of developing a computer method for calculating HF ionospheric transmission losses. In the course of the development of this method, a search of the literature was made to find suitable formulas that would permit the calculation of transmission losses due to lower ionosphere absorption. Since the primary interest was in total lower ionosphere absorption, no attempt has been made here to separate absorption losses into D- and E-region components. Such a separation has been attempted by others (Bibl and Rawer 1951; Bibl, Paul, and Rawer 1959; Rawer 1960b; Bibl, Paul, and Rawer 1961); however, theoretical results from these separations have been criticized on experimental grounds (Fejer 1961). The authors feel that in principle there are certain advantages in separating absorption losses into various components, but that in practice the separation techniques are not yet sufficiently developed to permit analyses similar to the ones performed in this paper.

The search of the literature revealed that although there has been much work on the theory of ionospheric attenuation of HF transmissions, little has been done in this country to develop formulas and techniques for calculating quantitatively the transmission losses involved. Even so, of the few formulas that were found in the literature, none gave results which agreed with observations made at equatorial latitudes. Consequently, to produce an acceptable computer method for calculating transmission losses, it became necessary for the present authors to develop absorption formulas valid for low and middle latitudes. This involved the analysis of a large amount of original published absorption measurements taken at stations widely separated in latitude. The results of the analysis are given in this paper.

Finding original published absorption measurements was difficult for several reasons. First, long series of continuous absorption measurements taken over one or more solar cycles are rare. Second, the majority of absorption measurements have been made at middle latitudes, with the result that very little data exist for equatorial latitudes. In addition, for those stations for which long periods of continuous data existed, the data were not always available in the same continuous series of publications. In the case of Freiburg, for example, absorption data have been published in the following series: (1) from 1948 to 1951 as part of the regular monthly station bulletin; (2) from 1952 to 1955 in a single report (which was published in 1956), and (3) since the year 1956 in the present publication form of a

separate absorption bulletin. For other stations the recording of absorption measurements has not always meant that the observed data were published. In the case of Singapore, for example, the authors used some unpublished data.

Because of the above difficulties encountered in obtaining the published values of the original measurements, and since these values may be of use in future studies, all of the data analyzed in this paper have been reproduced in the appendix. These data are the published monthly median midday [1] A-values for the stations, Slough, Freiburg, Singapore, and Dakar. The latitudes of these stations, the years for which data were published, the total amount of available data, and the range of sunspot numbers (SSN) over which data were observed are given below in table 1.

TABLE 1.—*Equatorial ionosphere absorption data used in this report*

Station	Latitude	Period of absorption measurements	Years of data available	Range of SSN (monthly mean)
Slough	51°31′N.	1935–1953	18½	0–201
Freiburg	48°06′N.	1949–1961	13	0–254
Dakar	14°36′N.	1951–1955	4½	0–109
Singapore	1°19′N.	1949–1954	5	0–144

The sources of the above data are given in the appendix, page 29.

The purpose of this paper is: (1) to analyze and discuss the seasonal and solar cycle variation of absorption at the stations, Slough, Freiburg, Dakar, and Singapore; (2) to examine the latitudinal variation of absorption not due to the $\cos^n \chi$ variation (χ is the solar zenith angle, n is a constant for a given location); (3) to develop formulas for calculating HF transmission losses due to lower ionosphere absorption which separately take into account seasonal variation of absorption with latitudinal effects, latitudinal and solar cycle variation of absorption, and winter anomaly effects; and (4) to give in one publication, for the convenience of possible future studies, all of the midday absorption data analyzed in this paper.

In this paper, a brief description is given concerning the theory of lower ionosphere absorption and the procedure for taking absorption measurements. The seasonal variation of absorption is discussed in detail for the four ionosphere stations: Slough, Freiburg, Dakar, and Singapore. Quantitative formulas are given for calculating the seasonal variation at these stations. The equatorial and winter anomalies are also treated. The solar cycle variation of absorption is given, and formulas are derived for calculating this variation as a function of sunspot number. The results obtained for seasonal variation of absorption, equatorial and winter anomalies, and the solar cycle variation are combined into formulas. These results are compared with published results obtained by other authors. The latitudinal variation of absorption not due to the variation in $\cos \chi$ is discussed next. This type of variation was an unexpected result of the data analysis, and to the best of our knowledge, has not been discussed previously in the literature. An empirically derived formula is given for calculating transmission losses due to lower ionosphere absorption that separately takes into account the effects of: (1) seasonal variation with latitudinal effects, (2) latitudinal variation, (3) solar cycle variation, and (4) winter anomaly effects. Finally, the results are extended to oblique and nighttime absorption. The appendix contains the published monthly median midday values of the absorption data analyzed in this paper, together with the sources of the data. In addition, tables of various quantities derived during the course of the data analysis are also summarized for convenience in the appendix.

LOWER IONOSPHERE ABSORPTION COEFFICIENT AND ABSORPTION INDEX

Two main methods are generally used for measuring lower D- and E-region ionospheric absorption. They are the reflection method of vertical incidence sounding, and the riometer method of measuring changes in cosmic noise. This paper is concerned only with absorption measurements obtained from vertical incidence soundings.

The reflection method gives the apparent reflection coefficient ρ of the ionosphere. The method and the operating techniques involved are discussed elsewhere (Piggott 1953; Piggott et al. 1957). We now give a brief outline of the classical theory for the determination of the D-region absorption by the pulse reflection method. The Sen-Wyller (1960) presentation is not used because we believe that the pulse reflection method is not precise enough to warrant this more sophisticated treatment.

The real refractive index μ and absorptive index χ are given as follows (Budden 1961, p. 172):

[1] In the case of Dakar, all of the A-values from October 1951 through December 1955 were obtained at 1040 local time.

$$\mu^2-\chi^2=1-\frac{\omega_p^2}{\omega^2+\nu^2} \tag{1}$$

$$2\mu\chi=\frac{\nu}{\omega}\frac{\omega_p^2}{\omega^2+\nu^2} \tag{2}$$

where ω_p is the angular plasma frequency, ω is the angular wave frequency, and ν is the collision frequency. Combining equations (1) and (2) gives the absorptive index χ as

$$\chi=\frac{\nu}{2\omega}\frac{1}{\mu}(1-\mu^2+\chi^2). \tag{3}$$

The absorption coefficient k occurs in the exponent of the exponential damping factor of the electric field vector of the radio wave. It is proportional to the absorption index and is given by

$$k=(\omega/c)\chi. \tag{4}$$

Using the approximation (nearly always valid in the lower ionosphere) that $\chi^2 \ll 1-\mu^2$ (Budden 1961, p. 173), the absorption coefficient is given by (Ratcliffe 1962, p. 38) as,

$$k=\frac{\nu}{2c}\frac{1-\mu^2}{\mu}, \tag{5}$$

or

$$k=\left(\frac{2\pi e^2}{mc\epsilon_0}\right)\frac{1}{\mu}\frac{N_\nu}{(\omega\pm\omega_H)^2+\nu^2}, \tag{6}$$

where N is the electron density, ω_H is the gyrofrequency, c is the velocity of light, ϵ_0 is the dielectric constant of free space, and e and m are the electron charge and mass, respectively. The plus and minus signs in equation (6) are associated with the ordinary and extraordinary waves, respectively. Throughout the remainder of this paper, we consider only the absorption of the ordinary wave.

To obtain the total absorption of an electromagnetic wave propagating via the ionosphere, it is necessary to integrate the absorption coefficient along the ray path. Thus, for a radio wave emitted with amplitude E_0 at some reference distance from a transmitter, the amplitude of the wave reflected vertically from the ionosphere is given by

$$E_1=\frac{E_0}{2h'}\exp\left(-2\int_0^h k(z)dz\right), \tag{7}$$

where h' and h are the virtual and true heights of reflection, respectively (Whitehead 1958; Ratcliffe 1962, p. 402). The amplitude E_1 of a radio wave reflected from the ionosphere is also given by (Ratcliffe 1962, p. 402)

$$E_1=\frac{E_0}{2h'}\rho, \tag{8}$$

where ρ is the apparent reflection coefficient of the ionosphere. Therefore, the amplitude of the reflection coefficient of the ionosphere is given by

$$\rho=\exp\left(-2\int_0^h k(z)dz\right) \tag{9}$$

(see Budden 1961, p. 325, for a discussion of the phase of the reflection coefficient). In units of decibels, the attenuated power is given as $-20\log_{10}\rho$ which is equal to $-8.7\log_e\rho$.

In practice, the reflection coefficient is measured each day at noon on several frequencies, usually between 2 and 5 MHz. The method and the operating techniques involved are discussed by Piggott (1953) and Piggott et al. (1957). Since the absorption coefficient is proportional to $N\nu/\omega\pm\omega_H)^2$ if $(\omega\pm\omega_H)^2 \gg \nu^2$ (see equation (6)), a plot of $\log_{10}\rho$ versus $(\omega\pm\omega_H)^2$ will show whether or not the assumptions underlying equation (8) are valid. Employing these considerations, a graphical technique is used (Piggott 1953) to eliminate those values of ρ thought to be influenced by the occurrence of deviative absorption. The graphically derived result is the absorption index A, which is independent of frequency and which gives a useful index of the nondeviative absorption in the lower ionosphere. The absorption index A is related to the reflection coefficient ρ by the relation

$$A(\text{dB MHz}^2)=8.7\ (f+f_H)^2\log_e\rho, \tag{10}$$

where f_H is the gyrofrequency (Appleton 1937).

The absorption index A is used to obtain the absorption at vertical incidence on other frequencies not too near the critical frequency of an ionized region (i.e., for frequencies at which deviative absorption is not significant). The formula used to calculate this transmission loss L_a in decibels is given by

$$L_a(\text{dB})=A/(f+f_H)^2, \tag{11}$$

where A is the absorption index.

For oblique incidence propagation, the value of absorption obtained from equation (11) is multi-

plied by a factor secant ϕ, where ϕ is the angle of incidence at the midpoint of the absorbing region. In using this simple procedure, however, caution should be exercised in situations involving multiple hops, because the absorption index is usually obtained only from first order reflections from the E and F regions. Later in this paper, the modification of the vertical incidence formula for the case of oblique incidence is discussed in greater detail.

To calculate the absorption for times other than noon, equation (11) is multiplied by a diurnal variation factor $(\cos 0.893\chi/\cos 0.893\chi_{12})^d$. The quantity χ_{12} is the solar zenith angle in degrees at local noon, and χ is the solar zenith angle at the time of the calculation. The factor 0.893 determines the sunset and sunrise times at a height of 100 km above the earth. The experimental value of the exponent d is of the order of unity (Taylor 1948) with values ranging from 0.6 to 1.3 being reported (Appleton and Piggott 1954). The reported values, however, are based upon a sunrise-sunset factor of unity rather than 0.893.

The general expression for the absorption losses of an obliquely incident wave propagating via the ionosphere is given by

$$L_a(\text{dB})=A(\text{dB MHz}^2)\left[\frac{\cos 0.893\chi}{\cos 0.893\chi_{12}}\right]^d \frac{\text{secant }\phi}{(f+f_H)^2}, \quad (12)$$

where the symbols have their previously defined meanings. All of the quantities in equation (12) except A, can be calculated from the geometry of the ray path. The index A depends upon the electron density and collision frequency profiles, and therefore, A must be determined empirically. This determination is made in the next section. In the latter part of this paper, the denominator term containing the frequency is modified to take into account absorption losses when the angular wave frequency ω is comparable to the collisional frequency ν.

THE GEOGRAPHIC AND TEMPORAL VARIATION OF THE ABSORPTION INDEX

The measured midday values of the absorption index A exhibit a short-term, annual variation and a long-term, 11-year variation. The short-term variation is due to the seasonal change of the solar zenith angle, and the long-term variation is due to the sunspot cycle. These two variations are illustrated in figures 1 through 4. In these figures, the published monthly median midday [2] values of A are shown for the stations, Slough, Freiburg, Singapore, and Dakar. In addition, the 13-month smoothed A-values and the 13-month smoothed sunspot numbers are also given; these are designated A_{13} and R_{13}, respectively. For convenience the A-values, and in addition the A_{13}-values are given in the appendix.

The annual variation of the A-values (i.e., variation of the nondeviative absorption) is due to the seasonal changes in the solar zenith angle. For Slough and Freiburg, maximum absorption occurs during the summer months (figs. 1 and 2), but for Singapore and Dakar, maximum absorption occurs slightly after the overhead transit of the sun. Because these stations are at equatorial latitudes, maximum absorption occurs twice a year (figs. 3 and 4).

The 11-year variation of absorption is related to the 11-year variation of the sunspot cycle. This solar cycle variation is illustrated in figures 1 through 4 by the R_{13}-curves. The year-to-year variation of the A-values is obtained as a running average of the A-values over a seasonal cycle (13 months). This year-to-year variation is also shown in figures 1 to 4. It can be seen that the correlation between the curves of absorption and solar activity is very good.

Thus, we see that absorption values for each ionosphere station undergo two different variations: (1) a seasonal variation and (2) a solar cycle variation. These variations are now determined quantitatively.

ANALYSIS OF THE SEASONAL VARIATION OF ABSORPTION

Observations indicate (Best and Ratcliffe 1938; Rawer 1949) and theory suggests (Appleton 1937; Nicolet and Bossy 1949) that the seasonal variation of absorption is given by

$$A=A_{13}K\cos^n\chi \quad (13)$$

where A_{13} is the 13-month running average of the A-values, χ is the solar zenith angle, and K and n are constants for a given station.

The parameters K and n in equation (13) are normally determined in the following manner. From the published A-values one obtains first the 13-month running average of the A-values (this is the average over one period of the seasonal variation).

[2] In the case of Dakar, the published A-values from October 1951 through December 1955 were obtained at 1040 local time. Noon values were estimated by multiplying the published values by the diurnal variation factor $\cos\chi/\cos\chi_{1040}=1.065$, taking the exponent $d=1.0$ in this case.

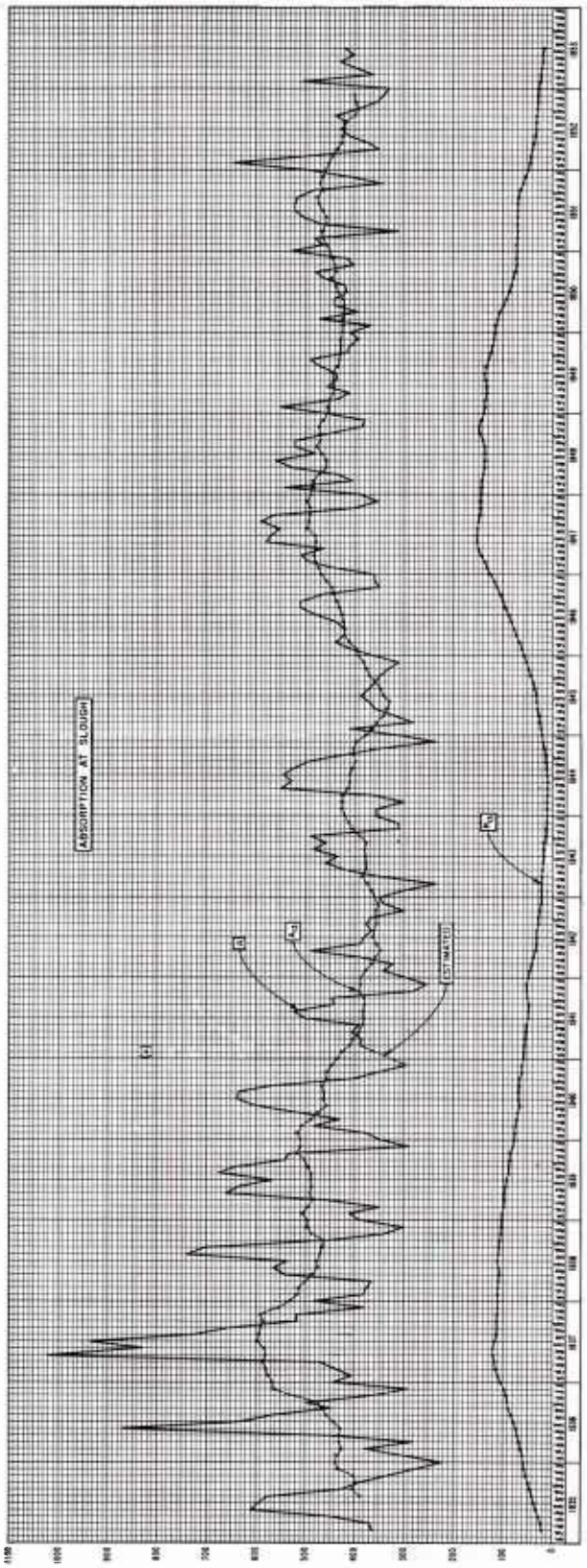

FIGURE 1.—Variation of the published monthly median midday values of the absorption index A. The quantity A_{13} is the smoothed, 13-month average of the A-values. R_{13} is the smoothed 13-month average of the sunspot numbers. This graph shows that maximum absorption occurs during the summer months and also at the maximum of solar activity.

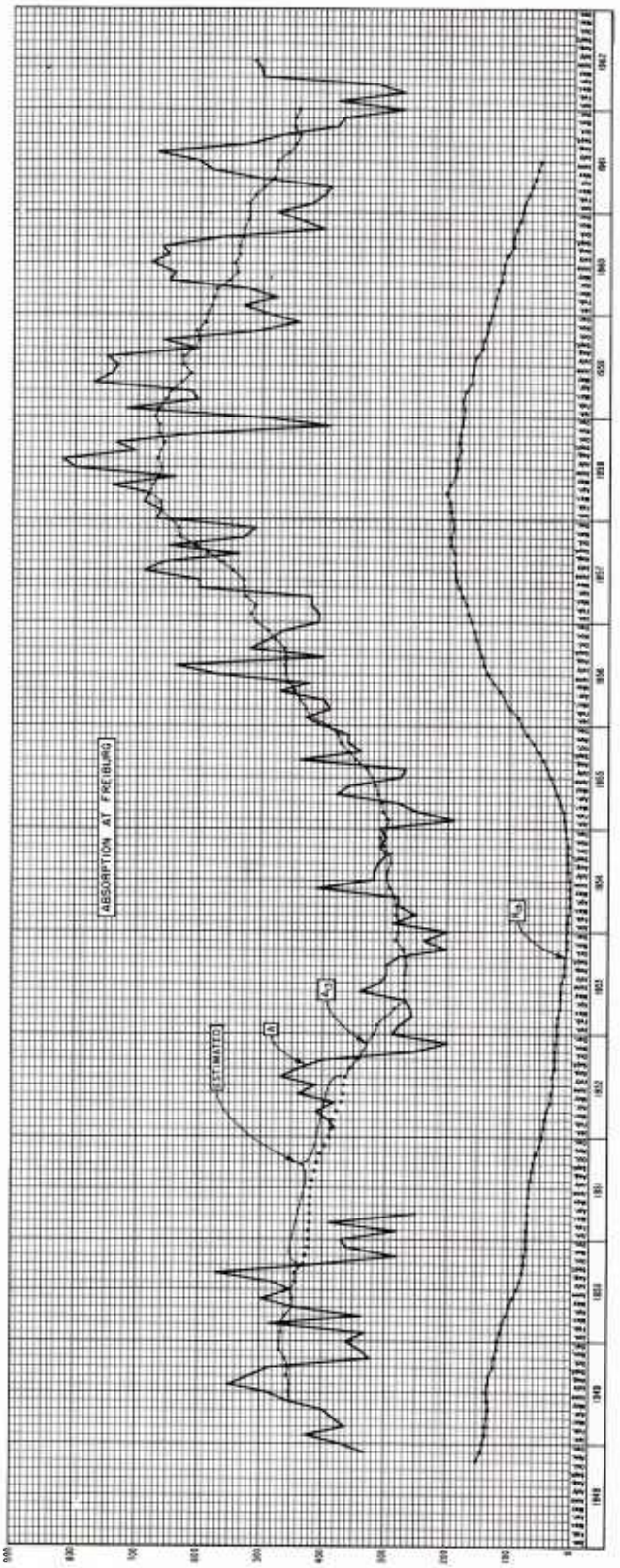

FIGURE 2.—Variation of the published monthly median midday values of the absorption index A. The quantity A_{13} is the smoothed, 13-month average of the A-values. R_{13} is the smoothed 13-month average of the sunspot numbers. This graph shows that maximum absorption occurs during the summer months and also at the maximum of solar activity.

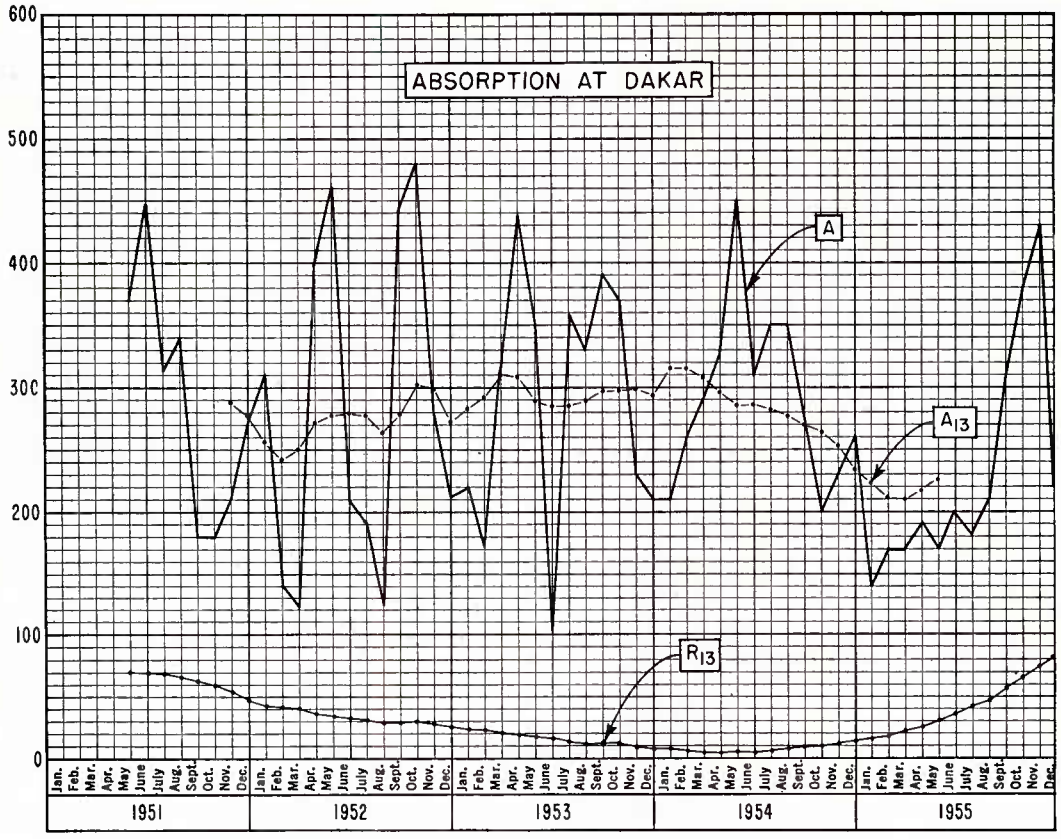

FIGURE 3.—Variation of the published monthly median midday values of the absorption index A. The quantity A_{13} is the smoothed, 13-month average of the A-values. R_{13} is the smoothed 13-month average of the sunspot numbers. The occurrence of the double maxima usually corresponds to the semiannual zenith passages of the sun.

Next each A-value is divided by its corresponding A_{13}-value; that is, for example, the January 1950 A-value is divided by the A_{13}-value for January 1950. The ratio A/A_{13} is designated I. Thus, a set of I-values is obtained, one for each month. Finally, the average of all the I-values for each month is calculated. These average I-values are designated $\bar{I}$. The quantities A, A_{13}, I, and $\bar{I}$ are given in tables A–I through A–IV of the appendix. For convenience the $\bar{I}$-values are also summarized below in table 2.

The variations of $\bar{I}$ with cos χ for the different stations are shown in figures 5 through 8. For the middle latitude stations, Slough and Freiburg, one notices that a *large* variation in cos χ results in a relatively *small* variation in absorption. More precisely, for Slough a 240 percent change in cos χ results in a 63 percent change in $\bar{I}$, and for Freiburg a 184 percent variation in cos χ corresponds to a 43 percent change in $\bar{I}$. Thus, at middle latitudes, the variation of absorption (i.e., the $\bar{I}$-values) is of the order of one-fourth the variation of cos χ.

In view of the above results, one would expect a small amplitude for the seasonal variation of absorption at equatorial latitudes, since the seasonal variation of cos χ is small at the Equator (i.e., the midday sun is almost always near the zenith). However, instead of the small amplitude variation of the

TABLE 2.—*Summarization of* I-*values*

	$\bar{I}=\overline{A/A_{13}}$			
	Slough	Freiburg	Singapore	Dakar
Jan.	0.990	0.876	0.940	0.822
Feb.	0.886	0.901	0.973	0.699
Mar.	0.881	0.881	1.052	0.806
Apr.	1.138	1.086	1.089	1.225
May	1.208	1.142	1.023	1.326
June	1.180	1.140	0.889	0.770
July	1.211	1.160	0.865	1.067
Aug.	1.147	1.104	1.004	0.954
Sept.	1.035	1.063	1.085	1.299
Oct.	0.826	0.838	1.140	1.197
Nov.	0.740	0.806	1.035	0.838
Dec.	0.884	0.876	0.910	0.896

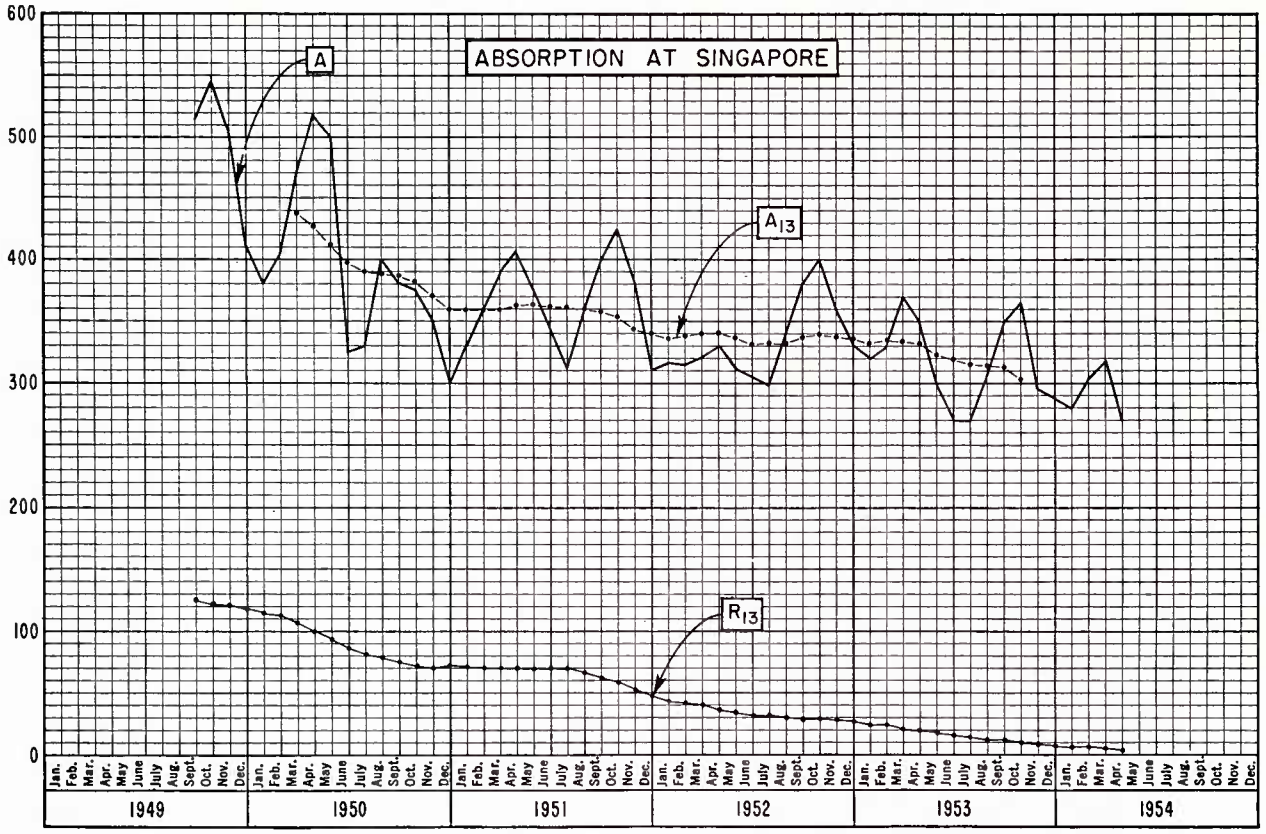

FIGURE 4.—Variation of the published monthly median midday values of the absorption index A. The quantity A_{13} is the smoothed, 13-month average of the A-values. R_{13} is the smoothed 13-month average of the sunspot numbers. The occurrence of the double maxima usually corresponds to the semiannual zenith passages of the sun.

order of one-fourth that of the variation of cos χ observed at middle latitudes, one finds an amplitude variation of approximately 3½ times the cos χ variation. For Dakar, for example, a change in cos χ of 28 percent is accompanied by a change of 89 percent in $\bar{I}$; and for Singapore the change in cos χ is only 9 percent, whereas the variation of $\bar{I}$ is of the order of 32 percent.

The abnormally large variation of equatorial absorption is somewhat unexpected, since the midday solar radiation is almost constant at these latitudes. This anomalous behavior was pointed out by one of the present authors several years ago (Delobeau and Gallet 1954). At that time, however, data were insufficient to determine quantitatively the magnitude of the variation (i.e., the value of the exponent n in the seasonal factor $\cos^n \chi$). With the data presently available, the calculation of the magnitude of the equatorial seasonal variation was performed. The results of these calculations are discussed later in the text.

In addition to the double maxima and minima seen in figures 7 and 8 for Singapore and Dakar, one also notices in each graph that both absorption maxima and one of the minima lag the cos χ curves by approximately 18 days (as determined from a cross-correlation analysis). This lag is of the order of the magnitude of the thermal lag observed just below D-region heights (Reed 1962), which is in all probability associated with the dynamics of the D region.[3] To take this delay into account for determining the seasonal variation of absorption, it was necessary to shift the values of $\bar{I}$ in figures 7 and 8 by an amount corresponding to 18 days. The values resulting from this translation are the ones used in the subsequent analysis.

To determine the seasonal variation of absorption for each station, standard logarithmic plotting procedure is used to transform the graphs of figures 5, 6, 7, and 8 into the form shown in figures 9 through 12. In these latter graphs, the systematic seasonal changes of absorption are readily seen by following the arrows from one month to the next (the numbers

[3] D-region dynamics also account for the abnormally large variations in the amplitude of the equatorial absorption mentioned above. A discussion of the mechanisms involved in D-region dynamics is given later.

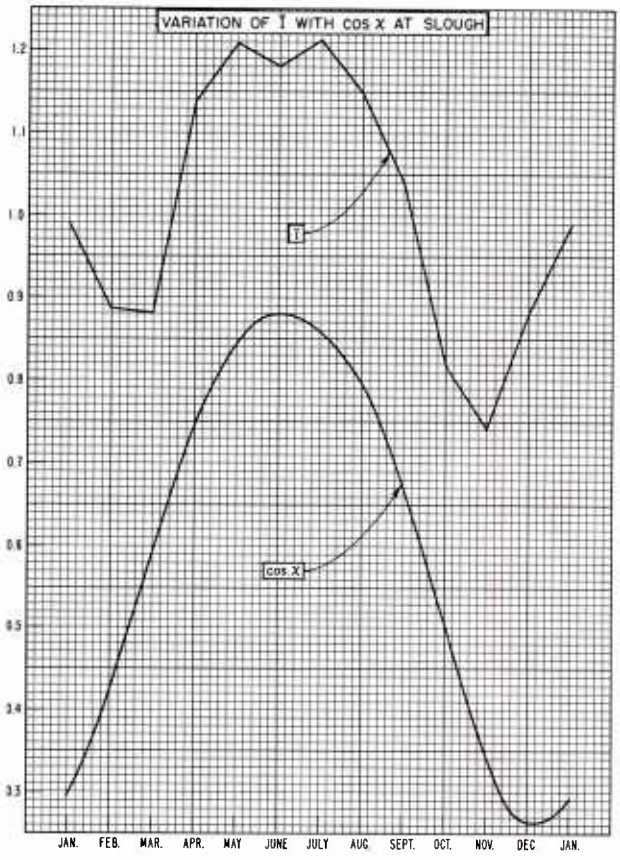

FIGURE 5.—Variation of absorption with cos χ. For a middle-latitude station, a large variation in cos χ results in a small variation of absorption.

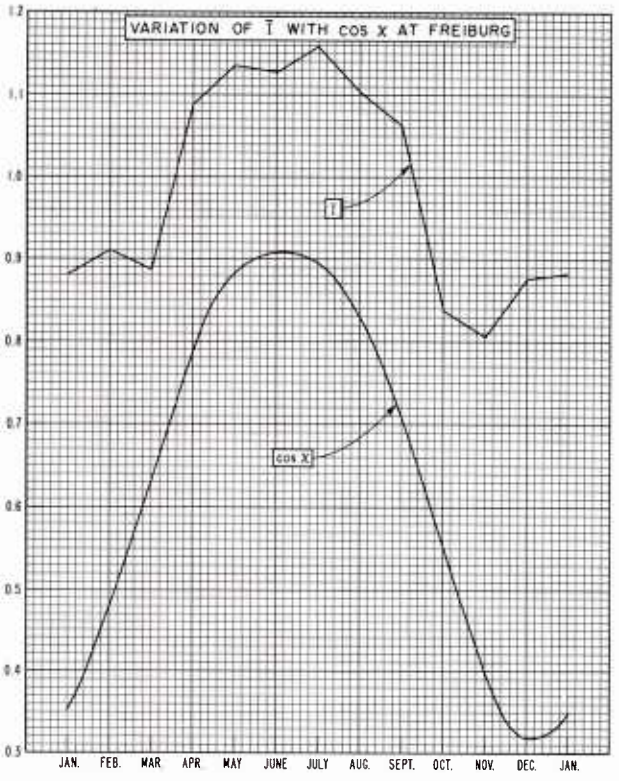

FIGURE 6.—Variation of absorption with cos χ. For a middle-latitude station, a large variation in cos χ results in a small variation of absorption.

in the figures represent months of the year—1 for January, 2 for February, etc.). Figures 9 through 12 were plotted as $\bar{I}$ versus $\frac{1}{2}\cos\chi$ in order to center the data in the graph.

The straight lines in figures 9 through 12 were determined by least-squares curve-fitting techniques. In the case of Slough and Freiburg, only the nonwinter months of March through October were used in determining the equations of the lines because of the winter anomaly phenomena discussed below. Using the Student t coefficient and assuming that the data are independent and normally distributed, the values of K and n were calculated (see equation (13)) for the four stations and are given below in table 3 together with 95 percent confidence limits for n. The lines in figures 9 through 12 were extrapolated beyond cos χ equal to unity in order to show the large changes in slope of the seasonal variation for the different stations.

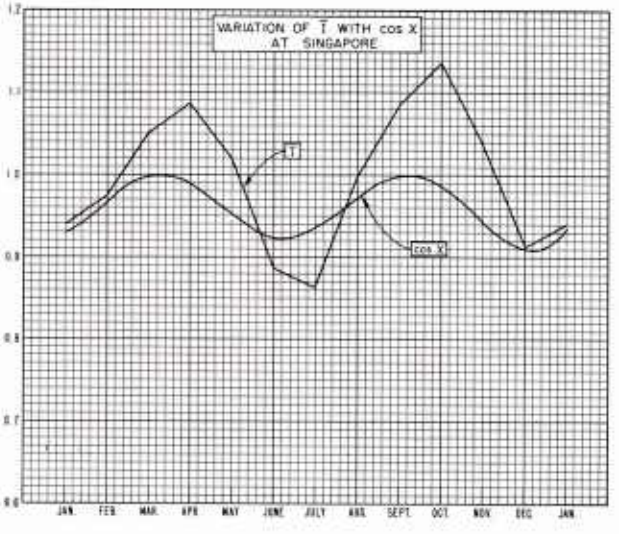

FIGURE 7.—Variation of absorption with cos χ. For an equatorial station, a small variation in cos χ results in a large variation of absorption (compare with figs. 5 and 6). Notice the pronounced lag of the maxima of $\bar{I}$ relative to the maxima of cos χ. There is also a slight lag in the minimum at July. The overall lag is of the order of 18 days (determined by a cross-correlation analysis).

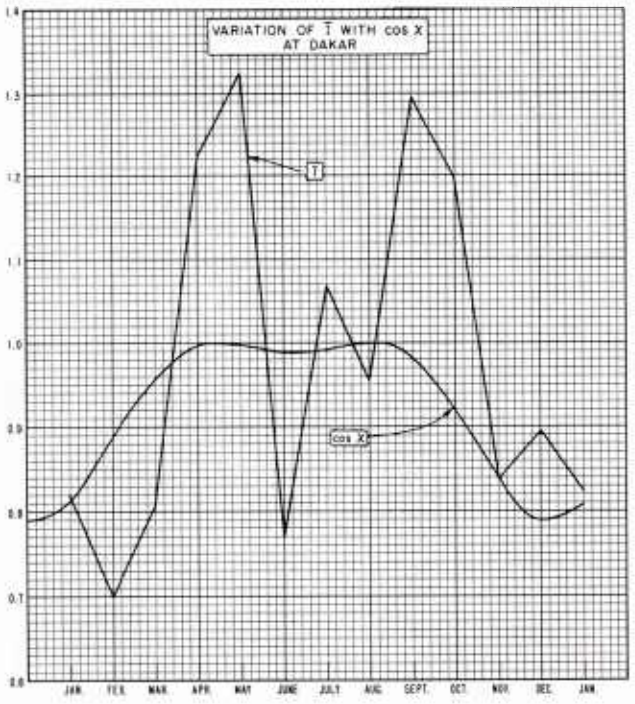

FIGURE 8.—Variation of absorption with cos χ. For an equatorial station, a small variation in cos χ results in a large variation of absorption (compare with figs. 5 and 6). Although not as apparent as at Singapore (fig. 7), an overall lag of approximately 18 days also occurs for this station.

TABLE 3.—*Empirical values of constants* K *and* n $I = K \cos^{n} \chi$

Station	K	n	95% confidence limits for n
Slough	1.35	0.72	$0.57 \leqq n \leqq .88$
Freiburg	1.25	0.66	$0.46 \leqq n \leqq .85$
Dakar	1.10	1.53	$0.64 \leqq n \leqq 2.43$
Singapore	1.10	2.40	$1.43 \leqq n \leqq 3.37$

Classical photoionization theory predicts a value of 1.5 for the exponent n for a simple Chapman-type absorbing region (Appleton 1937). For more realistic models of the D region, values of n less than 1.5 are always obtained (Nicolet and Bossy 1949; Appleton and Piggott 1954; Mitra and Jain 1963). Therefore, the values of n given in table 3 for Slough and Freiburg are not in disagreement with the theory. However, for the equatorial stations Dakar and Singapore, the observations are in disagreement with the theory—particularly in the case of Singapore.

Probably the reason that classical photoionization theory does not explain the abnormal amplitude of the seasonal variation of absorption at the Equator is because the theory does not take into account dynamic processes of the D region caused by geographical factors, meteorological effects, systematic seasonal variations of the ionosphere for different latitudes, and similar effects. These processes give rise to large-scale motions of air masses between the northern and southern hemispheres. These motions generally follow with a lag, the latitudinal position of the sun (Hess 1959). This horizontal motion produces turbulence which results in a mixing of the atmospheric constituents in the vicinity of the Equator. As a result of this mixing, electrons in the lower ionosphere are brought down to lower heights. This mixing results in an increase in the amount of absorption, since absorption is proportional to $\int \nu N_e dh$, where ν is the collision frequency and N_e the electron density; and since ν increases exponentially for decreasing heights in the ionosphere. (The above description is necessarily qualitative for two reasons. First, quantitative knowledge of atmospheric turbulence at D-region heights and the factors producing it are not available. Second, there is a scarcity of equatorial absorption measurements with which to compare observations with theory. Consequently, effects of turbulence on absorption are beyond the scope of the present paper.)

For Slough and Freiburg (figs. 9 and 10), the winter months of November, December, January, and February give proportionately more absorption than the nonwinter months. This is the well-known "winter anomaly" phenomena (Appleton and Piggott 1954). To account for the "winter anomaly" when using equation (13), it is necessary to use an empirical winter effect coefficient W. This coefficient is unity for all months except November, December, January, and February (the months of the "winter anomaly"). The value of W for these months is such that the observed values of absorption are obtained instead of the values given by the straight

TABLE 4.—*Average winter effect coefficient,* W, *for Slough and Freiburg*

Month	Slough	Freiburg	Average
November	1.14	1.18	1.16
December	1.64	1.48	1.56
January	1.69	1.39	1.54
February	1.18	1.17	1.18

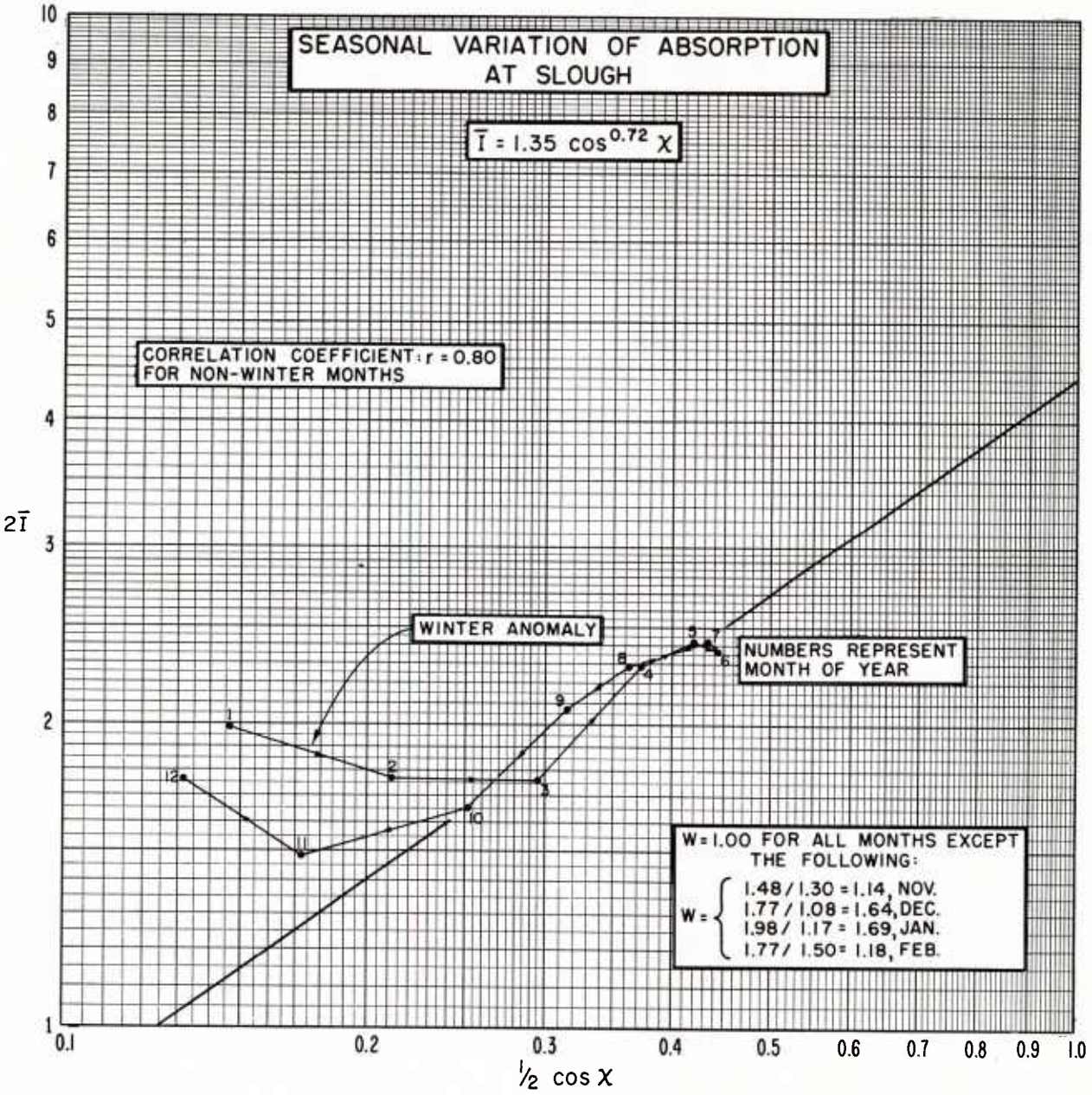

FIGURE 9.—Seasonal variation of absorption as a function of cos χ. The nonwinter months of March through October are seen to lie very close to the straight line (for these months the correlation coefficient equals 0.80). The winter months deviate markedly from the straight line; this is due to the winter anomaly effect.

lines in figures 9 and 10. The W-values of these four months are summarized in table 4 and are also included in figures 9 and 10.

Introducing the winter effect coefficient W results in the following expression for the seasonal variation of the A-values:

$$A = A_{13} K W \cos^n \chi \tag{14}$$

where for each of the stations the values of K and n are given in table 3, and for the middle latitude stations, the values of W are given in table 4.

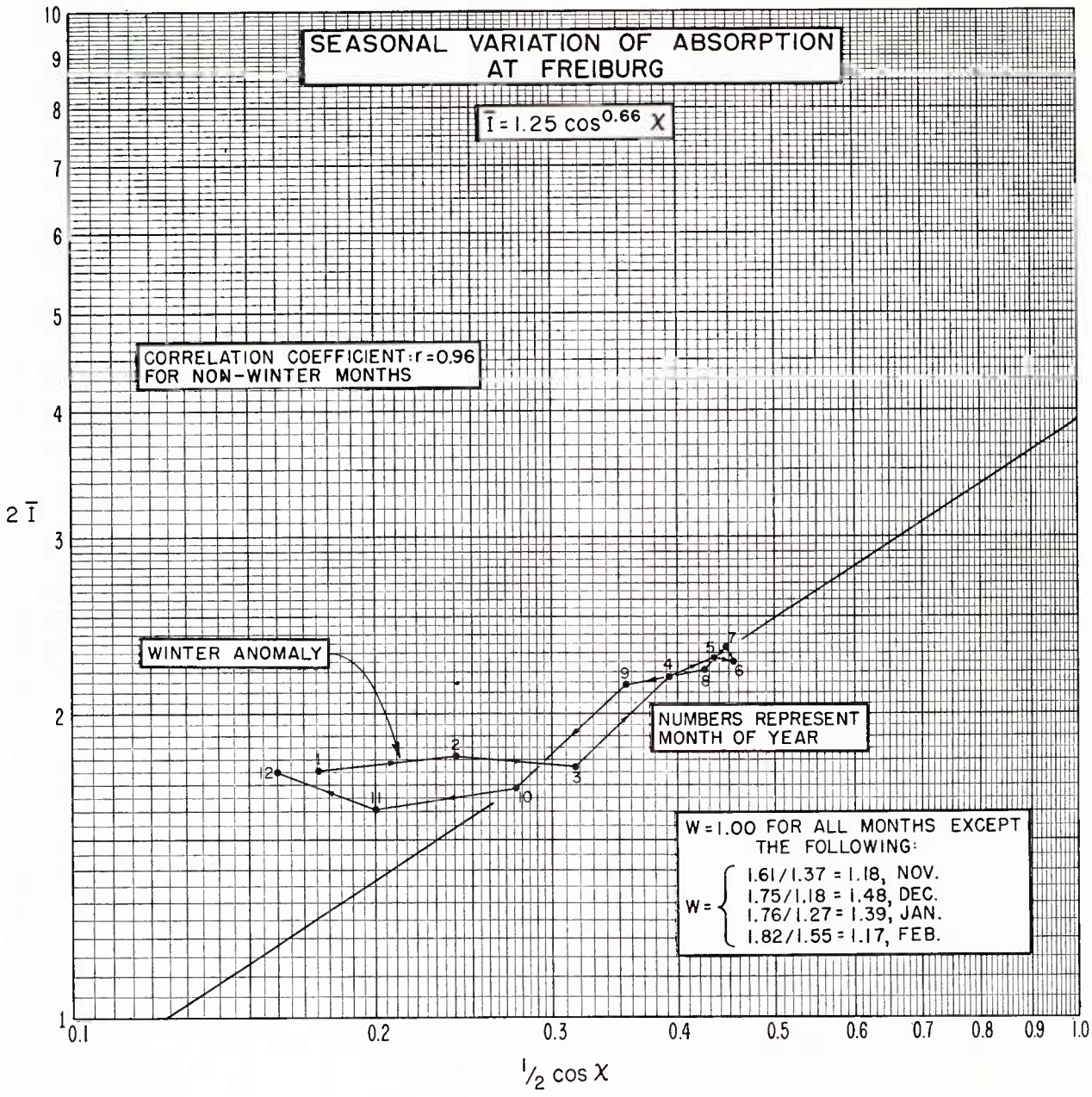

FIGURE 10.—Seasonal variation of absorption as a function of $\cos \chi$. The nonwinter months of March through October are seen to lie very close to the straight line (for these months the correlation coefficient equals 0.96). The winter months deviate markedly from the straight line; this is due to the winter anomaly effect.

387-150 O - 70 - 2

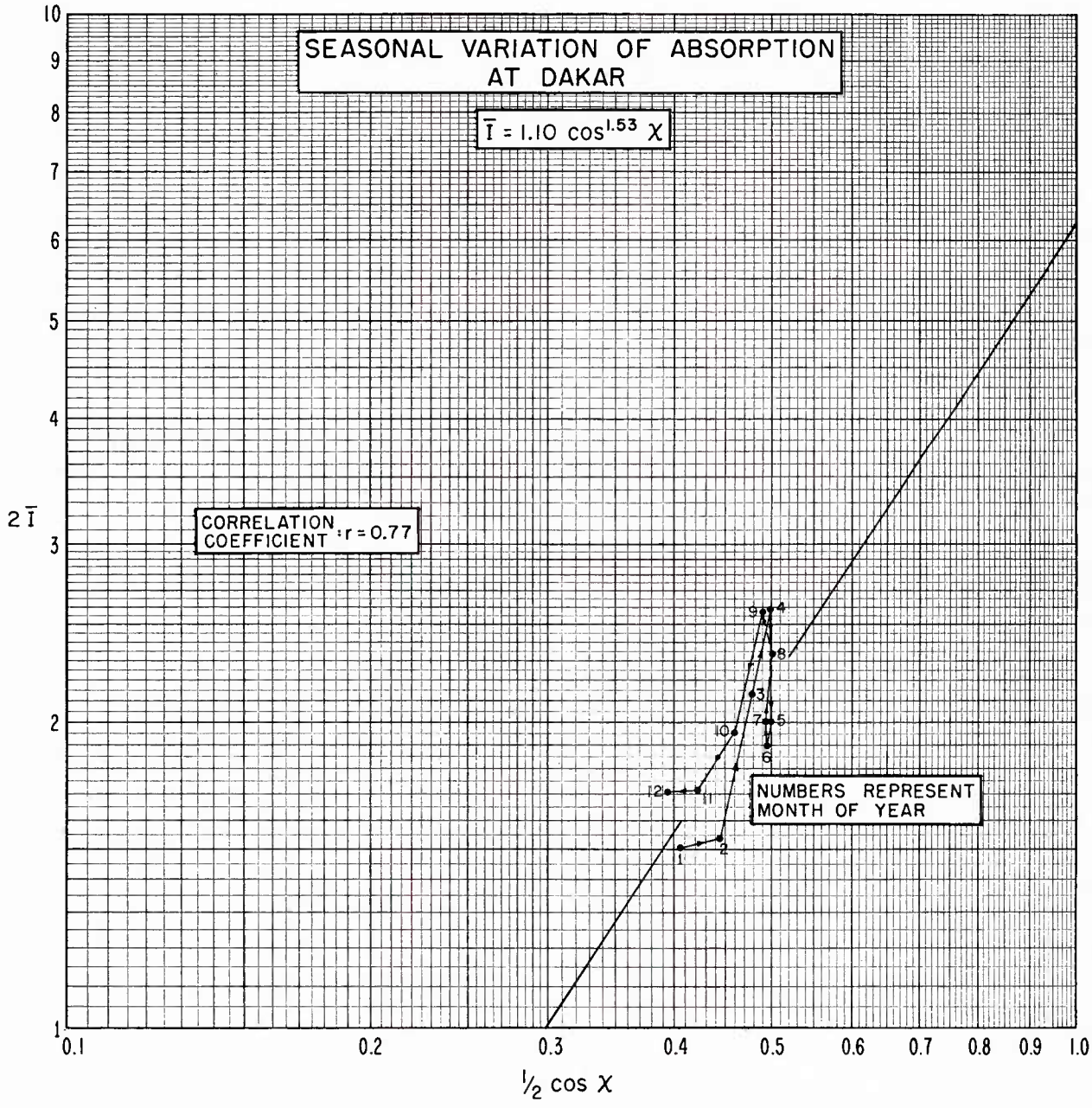

FIGURE 11.—Seasonal variation of absorption at Dakar.

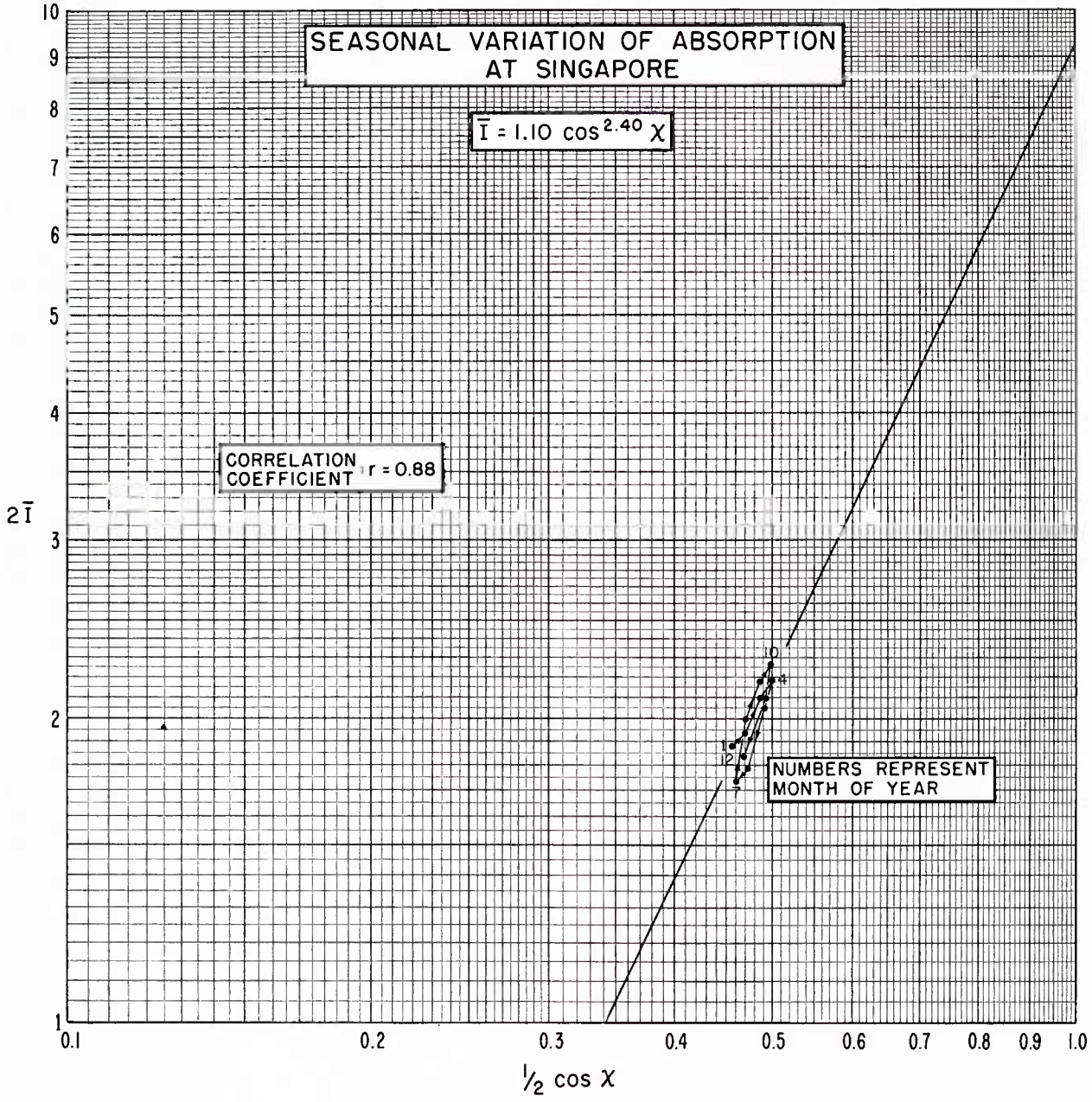

FIGURE 12.—Seasonal variation of absorption at Singapore.

ANALYSIS OF THE SOLAR CYCLE VARIATION OF ABSORPTION

In this section, the analysis of the variation of absorption with the sunspot cycle is discussed. This variation of absorption with the solar cycle is shown by plotting the smoothed absorption index values A_{13} as the ordinate with the smoothed sunspot values R_{13} as the abscissa. The resulting graphs are shown in figures 13 through 16. The Slough absorption series covered two solar cycles and was plotted for convenience on two graphs (figs. 13 and 14).

For Slough and Freiburg (figs. 13, 14, and 15), one notices that the absorption values are different for the ascending and descending phases of the solar cycle. In the case of Slough, the magnitude of the values are also seen to change from one solar cycle to the next (compare figs. 13 and 14). A similar behavior has been observed in the relationship between the critical frequency in the F_2 region, foF2, and sunspot number (Ostrow and PoKempner 1952).

To simplify as much as possible the final expression for the absorption index A, it was decided to use a single linear relation for all of the Slough data and a single linear relation from all of the Freiburg data. In the case of Singapore (fig. 16), one straight line is seen to give a good fit to all of the observed data. However, for Dakar (fig. 16), there are insufficient data to determine the nature of the relation between absorption and sunspot

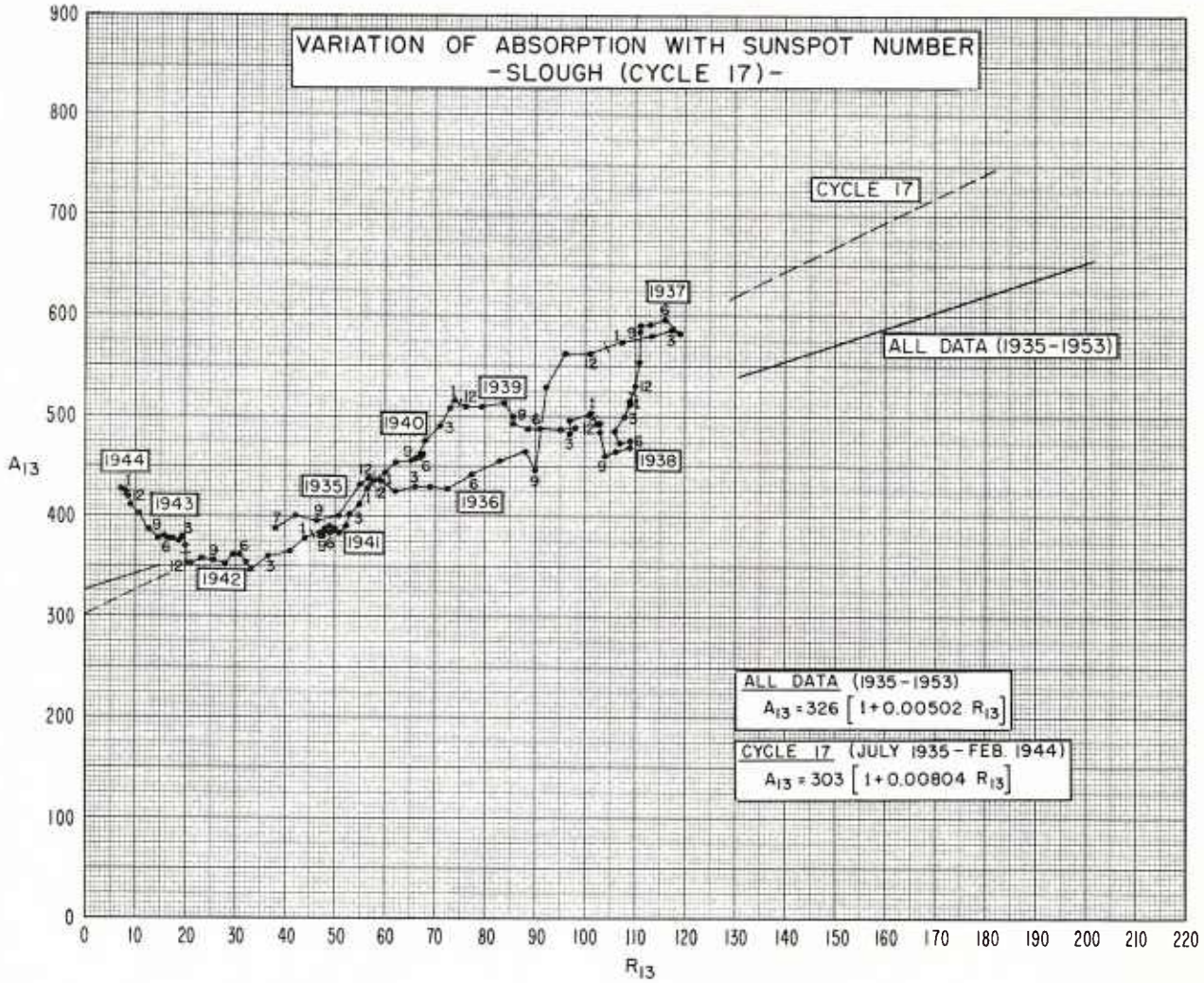

FIGURE 13.—Absorption as a function of solar activity for sunspot cycle 17. The straight lines give the linear relation of absorption with sunspot number. The dashed line gives the relation for cycle 17. The solid line gives the relation for the combined data of cycles 17 and 18 (see fig. 14).

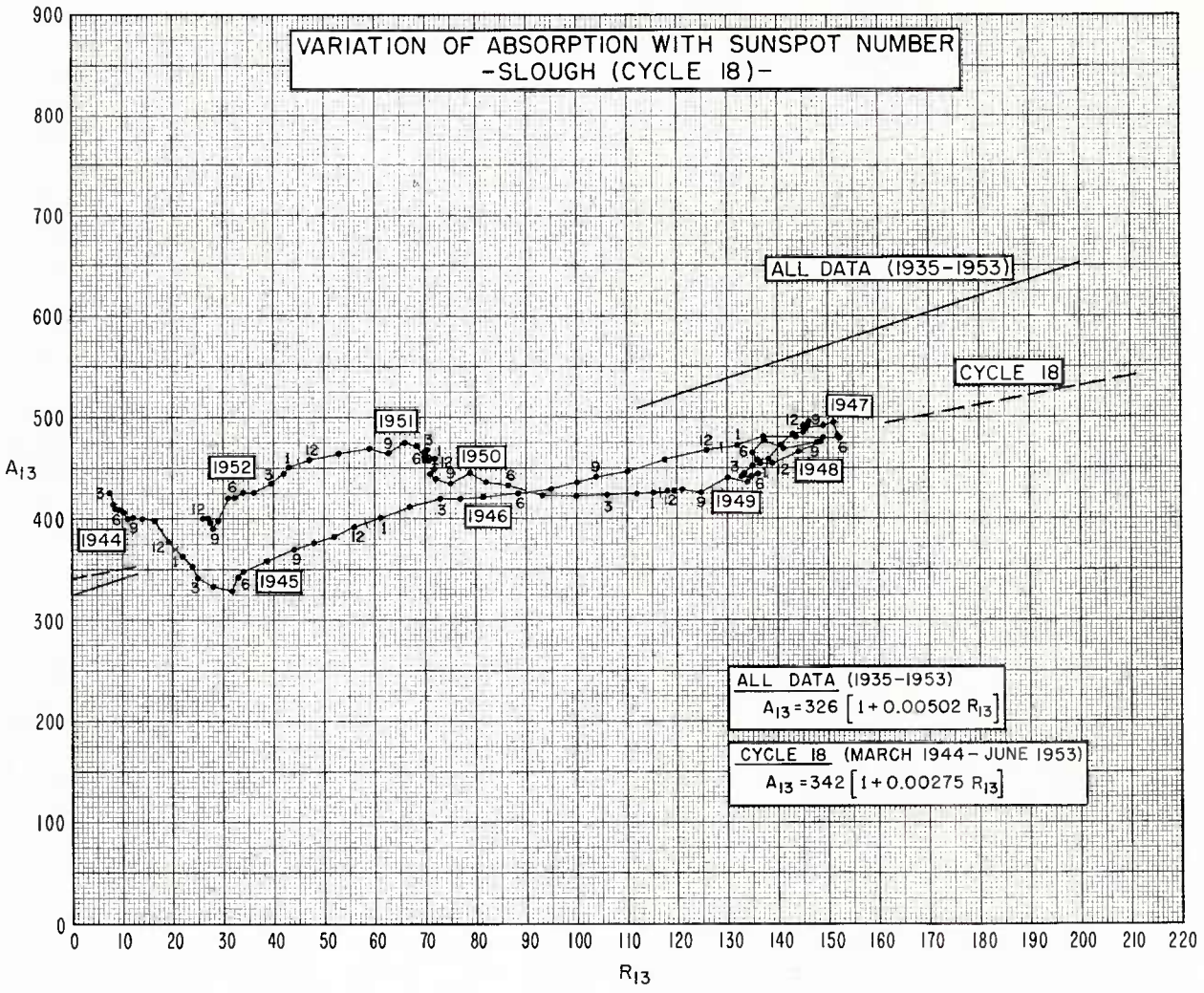

FIGURE 14.—Absorption as a function of solar activity for sunspot cycle 18. The straight lines give the linear relation of absorption with sunspot number. The dashed line gives the relation for cycle 18. The solid line gives the relation for the combined data of cycles 17 and 18 (see fig. 13).

number. For Dakar, only the value A_0 of absorption at sunspot minimum can be deduced—and then only approximately.

The expression relating absorption and sunspot number is assumed to be linear and is given by

$$A_{13}=A_0[1+bR_{13}] \tag{15}$$

The values of A_0 and b for the four ionosphere stations analyzed are given below in table 5 and are also given in the appropriate graphs of figures 13 through 16.

TABLE 5.—*Values of coefficients* A_0 *and* b

Station	A_0	b
Slough	326	0.00502
Freiburg	304	0.00550
Dakar	270	.....
Singapore	289	0.00443

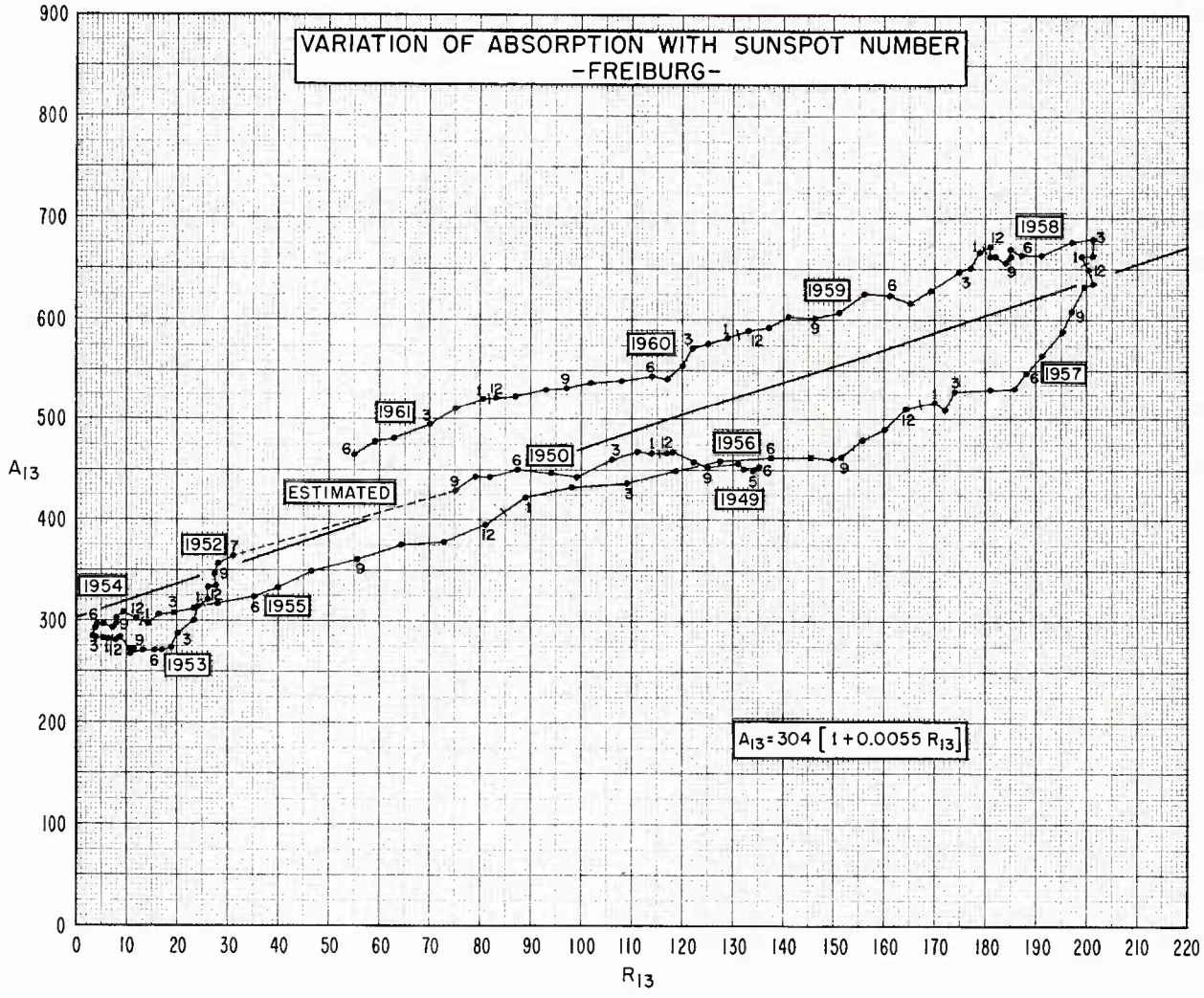

FIGURE 15.—Absorption as a function of solar activity. Notice the difference in absorption for the ascending and descending phases of the solar cycle.

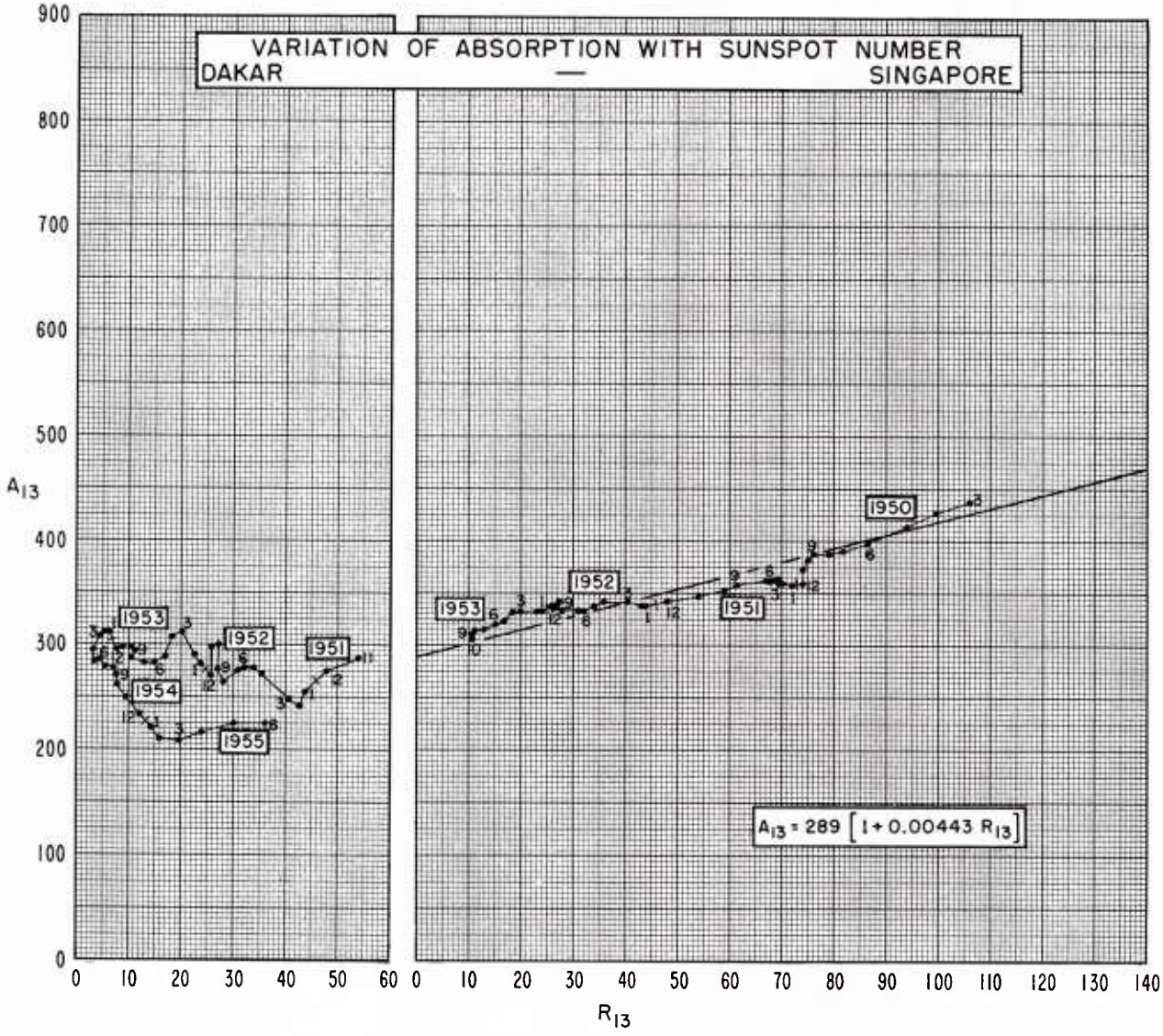

FIGURE 16.—Absorption at Dakar and Singapore as a function of solar activity.

SUMMARY OF STATION ANALYSES

In summarizing the results of the analyses for four ionosphere stations, the combined seasonal and solar cycle variation of the median midday A-values is given by (see equations (14) and (15))

$$A = A_0 K [1 + bR_{13}] W \cos^n \chi, \qquad (16)$$

where the numerical quantities are given in table 6.

The winter effect coefficient W is summarized in table 7.

TABLE 6.—*Empirical equations for ionospheric absorption at four stations*

Station	Latitude	$A = A_0 K [1 + bR_{13}] W \cos^n \chi$
Slough	51.5°N.	$A = 440\ [1 + 5.02\ (10)^{-3} R_{13}] W \cos^{0.72} \chi$
Freiburg	48.1°N.	$A = 380\ [1 + 5.50\ (10)^{-3} R_{13}] W \cos^{0.66} \chi$
Dakar	14.6°N.	$A = 295\ [1 + \ldots R_{13}] W \cos^{1.53} \chi$
Singapore	1.3°N.	$A = 318\ [1 + 4.43\ (10)^{-3} R_{13}] W \cos^{2.04} \chi$

COMPARISON WITH PUBLISHED RESULTS OBTAINED AT OTHER STATIONS BY OTHER AUTHORS

In this section the results of analyses by other authors are presented. These results were obtained from the literature on D-region absorption studies. Unfortunately, the amount of material dealing with seasonal variation is small, probably because most D-region studies have been concerned with the diurnal variation of absorption (not the concern of this paper). Since the present authors did not have access to the other authors' original measurements, only the results of their statistical analyses can be given.

The results of these analyses are summarized below in table 8.

The results in table 8 are in general agreement with the present authors results which are summarized in table 6.

TABLE 7.—*Winter effect coefficient*, W

For the months	Slough	Freiburg	Dakar	Singapore
March through October	1.00	1.00	1.00	1.00
November	1.14	1.18	1.00	1.00
December	1.64	1.48	1.00	1.00
January	1.69	1.39	1.00	1.00
February	1.17	1.17	1.00	1.00

LATITUDINAL VARIATION OF ABSORPTION

The coefficient A_0K and exponent n appearing in formula (16) should be independent of latitude if:

TABLE 8.—*Analyses of D-region absorption by other authors*

Station	Latitude	n	$b \times 10^3$	Period	References
Ibadan	7.4 °N.	0.90 (Sunspot MAX) 2.00 (Sunspot MIN)	2.6 (f=2.4 Mc/s) 3.4 (f=5.7 Mc/s)	1953 to 1958	Skinner and Wright 1961
Tsumeb	26.1 °S.	1.5		1957 to 1958	Umlauft 1961
Delhi	28.6 °N.	0.80 for D and E region 0.62 for D region		1958 to 1959	Rao, Mazumdar, and Mitra 1962
Prince Rupert	54.3 °N	0.50		1949 to 1958	Davies and Hagg 1955
Churchill	58.8 °N.	0.30		1955 to 1966	Peebles 1956
Baker Lake	64.3 °N.	0.10		1955 to 1956	Peebles 1956

(1) the D region is formed by uniform photoionization processes; and (2) the structure of the atmosphere at D-region heights does not change systematically with latitude. Examination of table 6 shows, however, that both the coefficient A_0K and the exponent n vary systematically with latitude.

The variation of A_0K with latitude is illustrated in figure 17. Assuming that the variation is linear (i.e., essentially assuming that Slough and Freiburg correspond to one observation, and that Singapore and Dakar correspond to another observation), the relation between A_0K and latitude λ is

$$A_0K = 286[1 + 0.0087\lambda] \tag{17}$$

where λ is the geographic latitude expressed in degrees.

The variation of n with latitude is illustrated in figures 18 and 19. Because of the limited amount of data available at equatorial latitudes, the confidence limits for n are very large for Singapore and Dakar. By comparison, the confidence limits for Slough and Freiburg are very narrow. The nature of the variation of n with latitude cannot be given with good accuracy, primarily because of the large confidence limits for the equatorial stations. As can be seen from figures 18 and 19, both a linear relation and a cosine relation fit the observed values equally well. The results illustrated in these figures indicate the inadvisability of using a single value of n for all latitudes—as is the practice of most prediction services (Rawer 1960a). We have chosen to use the linear relation because of its simplicity, and because it gives a cutoff in the seasonal variation

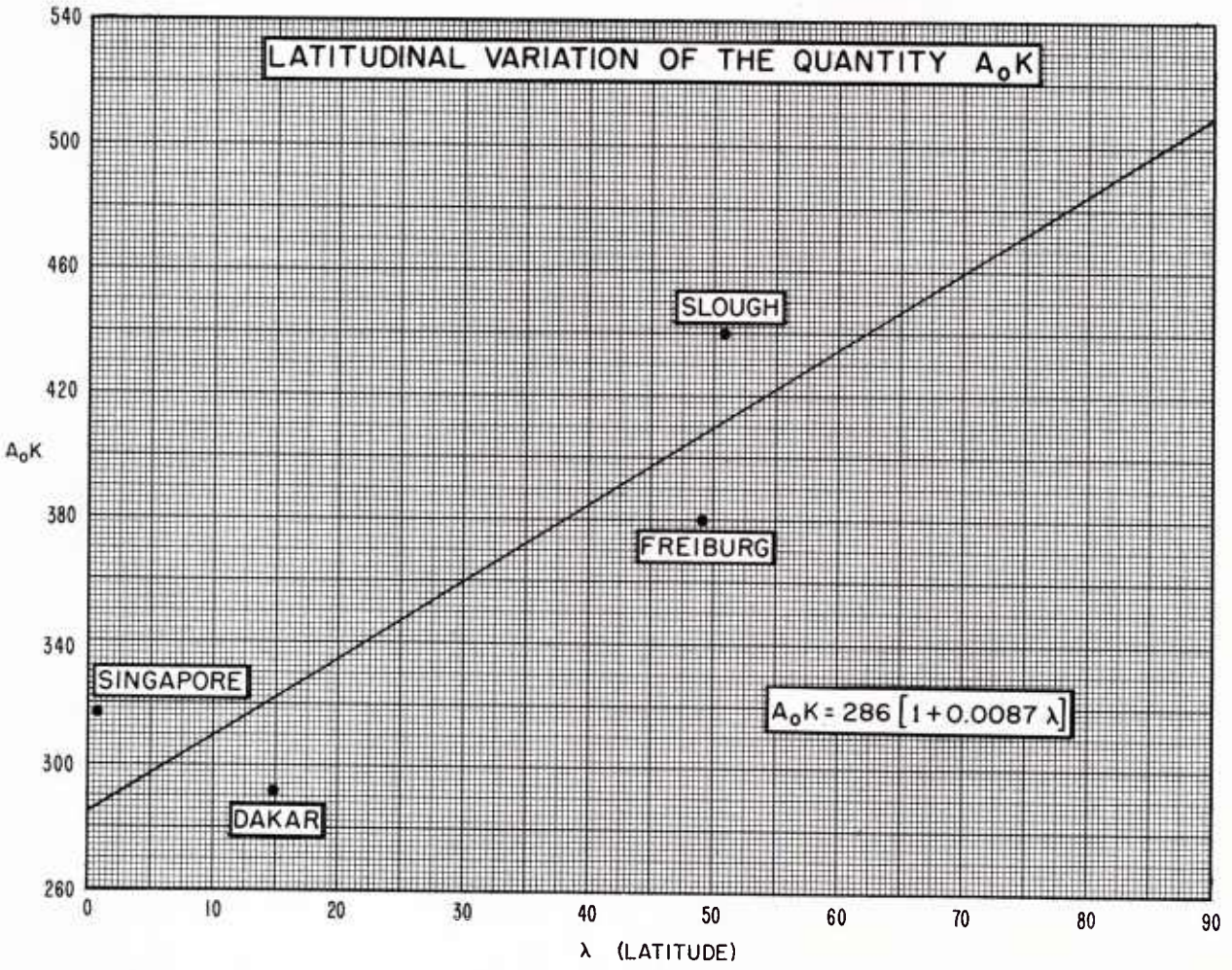

FIGURE 17.—Latitudinal variation of the amplitude of absorption excluding the variation due to cos χ.

387-150 O - 70 - 3

beyond the Arctic Circle. The linear variation of n is given by

$$n = 2.25 - 0.032\lambda \qquad (18)$$

where λ is the latitude expressed in degrees.

The linear and cosine curves given in figures 18 and 19 were obtained by a least-squares fit of the data from Singapore, Dakar, Freiburg, and Slough. In addition to the values for these stations, the values obtained by other authors' analyses (see preceding section) are also displayed in figures 18 and 19. As can be seen, these other results are not in disagreement with the present authors' results; and with the exception of the values for Ibadan and Delhi at sunspot maximum, all of the values are in good agreement with each other.

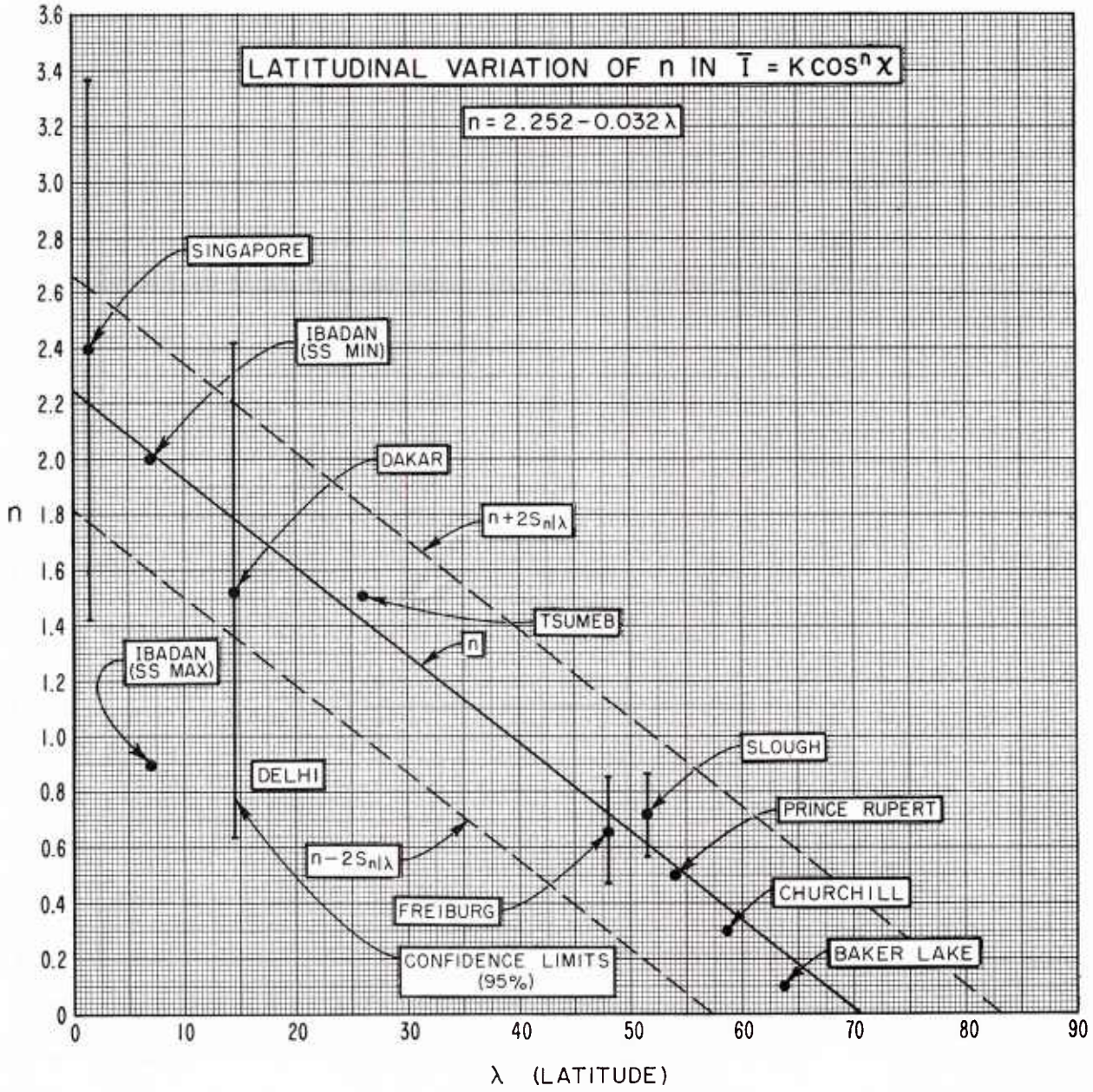

FIGURE 18.—Variation of the exponent n in the seasonal factor $\cos^n\chi$ as determined from the values from Singapore, Dakar, Freiburg, and Slough. The solid line gives the assumed linear variation with latitude. The dashed lines give the locus of values of two standard deviations from the solid line (i.e., $\pm 2S_{n|\lambda}$). The intervals on each of the station points are 95 percent confidence limits.

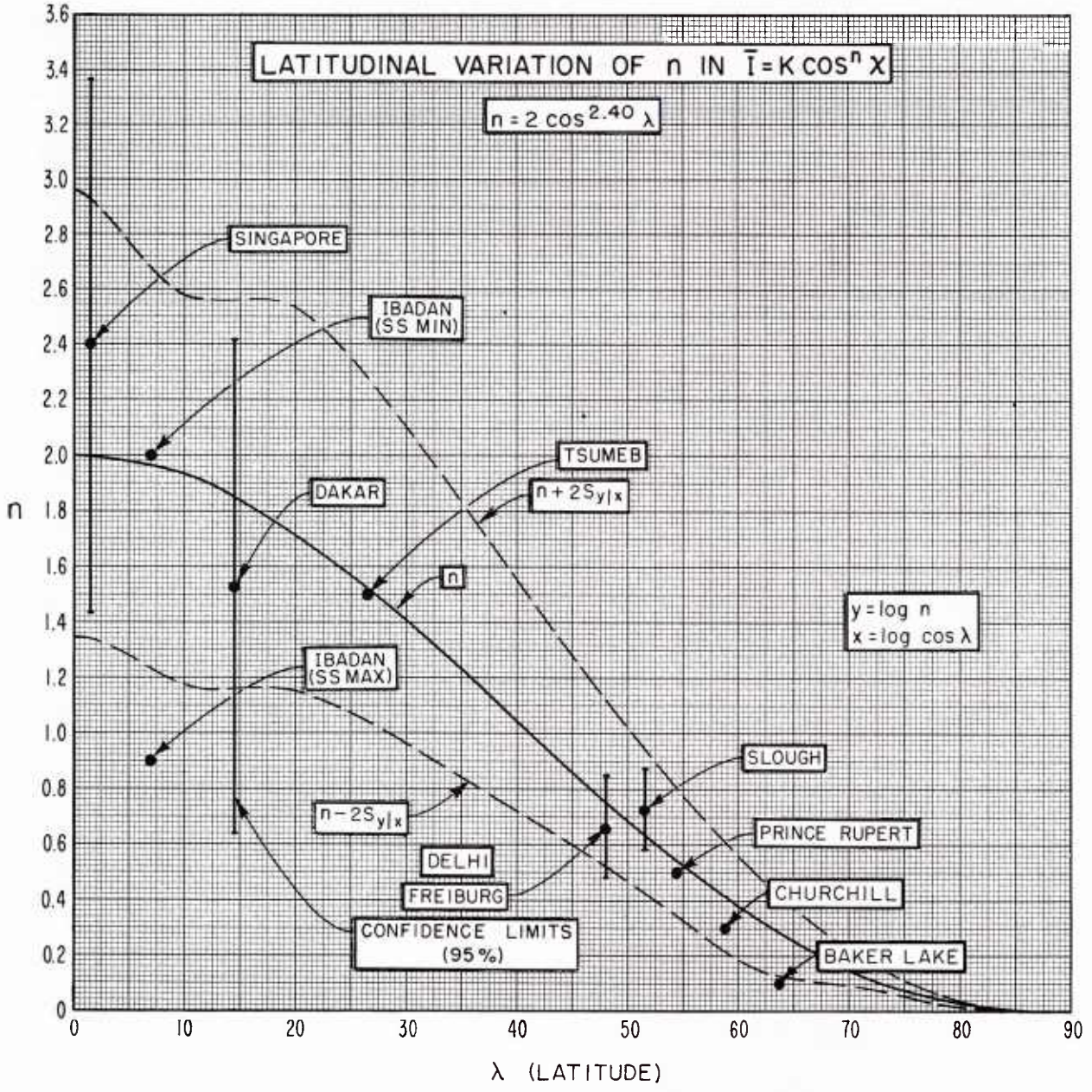

FIGURE 19.—Variation of the exponent n in the seasonal factor $\cos^n \chi$ as determined from the values from Singapore, Dakar, Freiburg, and Slough. The solid line gives the assumed cosine variation with latitude. The dashed lines give the locus of values of two standard deviations from the solid line (i.e., $\pm 2S_{n|\lambda}$). The intervals on each of the station points are 95 percent confidence limits.

At the present time, the latitudinal effects of the winter anomaly are not known. The W-factors different from unity appearing in tables 6 and 7 can probably be applied only within a certain range of geographic latitudes. In using the W-values, the following procedure is recommended: (1) apply the values only to latitudes above 30°, (2) use the average of the Slough and Freiburg values for latitude 60°, and (3) let these average values decline linearly north and south of 60° such that they have the value unity at latitudes 30° and 90°. Use a corresponding procedure during local winter in the southern hemisphere.

There does not seem to be any systematic variation with latitude of the coefficient b (see table 5). Consequently, the use of a constant value of b, say

$b = 0.005$, for all locations is recommended, or the appropriate station value, whichever is more convenient.

TABLE 9.—*The winter anomaly factor, W, for stations at or north of 30° latitude for all months*

Month	Latitude (λ)	W
Nov.	$30 \leq \lambda \leq 60$	$1.+0.0083\,(\lambda-30)$
Dec.	$30 \leq \lambda \leq 60$	$1.+0.0282\,(\lambda-30)$
Jan.	$30 \leq \lambda \leq 60$	$1.+0.0269\,(\lambda-30)$
Feb.	$30 \leq \lambda \leq 60$	$1.+0.0089\,(\lambda-30)$
Nov.	$60 \leq \lambda \leq 90$	$1.+0.0083\,(90-\lambda)$
Dec.	$60 \leq \lambda \leq 90$	$1.+0.0282\,(90-\lambda)$
Jan.	$60 \leq \lambda \leq 90$	$1.+0.0269\,(90-\lambda)$
Feb.	$60 \leq \lambda \leq 90$	$1.+0.0089\,(90-\lambda)$
All other cases.....		1.00

EMPIRICALLY DERIVED FORMULA FOR CALCULATING TRANSMISSION LOSSES

In deriving an overall formula for the calculation of the absorption index A which takes seasonal, solar, and latitudinal variations into account, a certain amount of accuracy is lost as compared to using individual formulas for each station. In spite of this disadvantage, however, there are numerous situations which warrant the use of a general formula. With this limitation in mind, we suggest the following formula for the total median lower ionosphere absorption at midday of a HF ionospheric propagation

$$L_a(\mathrm{dB}) = \frac{A(\mathrm{dB})}{(f+f_L)^2} \tag{19}$$

where f and f_L are given in MHz and where A is given by

$$A(\mathrm{dB}) = 286\,\underbrace{[1+0.0087\lambda]}_{\substack{\text{latitudinal}\\ \text{variation}}}\,\underbrace{[1+0.005R_{13}]}_{\substack{\text{solar cycle}\\ \text{variation}}}\,\underbrace{W}_{\substack{\text{winter}\\ \text{anomaly}\\ \text{effect}}}\,\underbrace{\cos^n\chi_{12}}_{\substack{\text{seasonal}\\ \text{variation}\\ \text{with}\\ \text{latitudinal}\\ \text{effect}}}. \tag{20}$$

where λ and χ_{12} are in degrees, $n = 2.25 - 0.032\lambda$ and W is given in table 9.

To calculate absorption for times other than midday, equation (10) is multiplied by a diurnal variation factor $[\cos 0.893\chi/\cos 0.893\chi_{12}]^d$. This factor is discussed on page 5 of the text.

Equation (20) differs from other formulas found in the literature in the following points: (a) there is an explicit latitudinal variation which does not depend on $\cos\chi$ and (b) the exponent of the seasonal variation factor $\cos\chi$ is a function of λ (rather than a constant for all latitudes).

CALCULATION OF OBLIQUE INCIDENCE ABSORPTION

Modification of Vertical Incidence Formula

For long-distance telecommunications, it is necessary to calculate the absorption of radio waves propagating obliquely via the ionosphere. As stated on page 4, it is the usual practice to multiply the vertical incidence absorption by a secant factor that is proportional to the angle of incidence of the wave at the absorbing region. This procedure would seem justified if the radio wave penetrated entirely the absorbing region; however, this situation does not always obtain at lower HF. Another difficulty that occurs at lower HF is that the wave frequency and the collision frequency are comparable. The net result is that oblique incidence absorption measurements below about 4 MHz do not follow an inverse square frequency law variation; that is, absorption proportional to the inverse second power of frequency. At the present time, it is not known how much of the observed discrepancy is due to the assumption of a secant of the angle of incidence variation and how much is due to the assumption of an inverse frequency variation. Since the collision frequency is not known to within a factor of about two, one normally uses an effective collision frequency. The present justification for the use of an effective collision frequency is that it compensates empirically for most of the discrepancies between observed and predicted oblique absorption values.

The previous considerations suggest that the vertical incidence formula (19) should be modified for oblique incidence absorption so that the formula becomes:

$$L_a(\mathrm{dB}) = \frac{A(\mathrm{dB\,MHz^2})\ \sec\phi}{\nu^2/4\pi^2 + (f+f_H)^2} \qquad (21)$$

where ν is the effective collision frequency. The additive term $\nu^2/4\pi^2$ in the denominator of equation (21) is significant when ν^2 is approximately equal to $(\omega+\omega_H)^2$, which occurs at lower HF. Values of the effective collision frequency obtained from oblique incidence data range from 18.3×10^6 sec^{-1} to $20.1\times(10)^6$ sec^{-1} (Josephson 1966; Lucas and Haydon 1966). The present authors determined a theoretical value of $20.2\times(10)^6$ sec^{-1} as follows. A plane electromagnetic wave is assumed incident upon the ionosphere given by the electron density profile and the collision frequency profile shown in figure 20. The assumed electron density model holds for

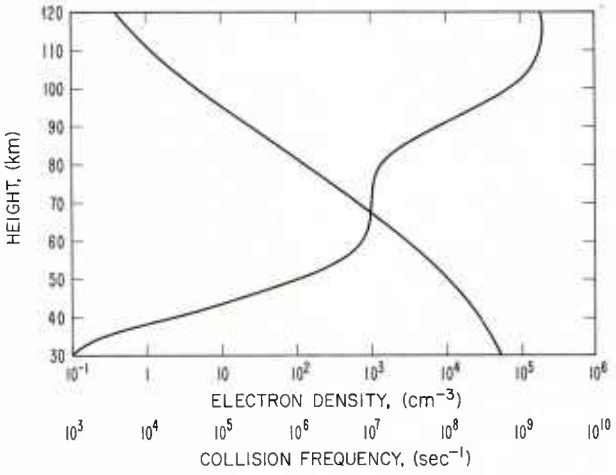

FIGURE 20.—Electron density and collision frequency profile used for the calculation of the absorptive index.

approximately sunspot maximum, and the collision frequency distribution is a fifth degree polynomial approximation to Nicolet's 1963 values. Using the Appleton-Hartree equation, the absorption index (see page 4) is calculated as a function of height for a frequency of 3 MHz and is plotted in figure 21. The absorption index has its maximum value at a height of 63 kilometers, and this corresponds to a collision frequency of $20.2\times(10)^6$ sec^{-1} (i.e., effective collisional frequency). For a plane wave at 30 MHz, the absorptive index peaks at 58 kilometers, and this corresponds to an effective collisional frequency of $40\times(10)^6$ sec^{-1} (fig. 21). At a wave frequency of 30 MHz, however, the effect of the additive term $\nu^2/4\pi^2$ is negligible (less than 5 percent change in the calculated absorption values).

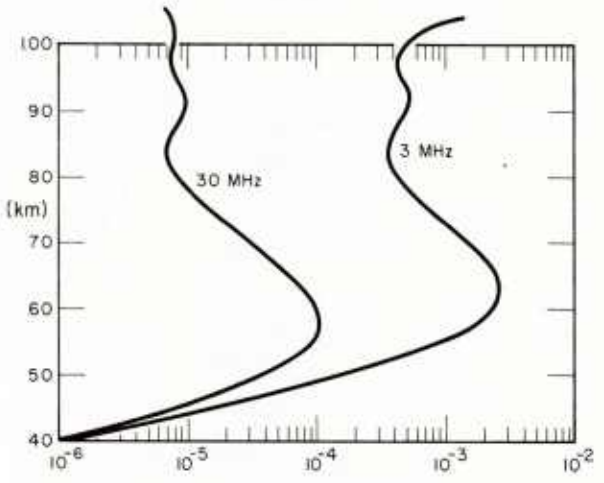

FIGURE 21.—Calculated absorptive index as a function of frequency and height.

Comparison Between Calculated and Observed Oblique Absorption Values

Equations (20) and (21) were used to calculate absorption values over the path between Long Branch, Illinois, and Boulder, Colorado, at midday for the months November 1958 through November 1959. Two sets of values were obtained corresponding to effective collision frequency values of 0 and $20\times(10)^6$ sec^{-1}, and these values are plotted in figure 22. The curve labeled A corresponds to a collisional frequency of zero (i.e., use of equation (19), and the curve labeled B was obtained from equation (21) with a collisional frequency of $20\times(10)^6$ sec^{-1}. During the observational period, an oblique HF and VHF propagation experiment was conducted over this path (Blair, Davis, and Kirby 1961), and included in the experiment was a transmission loss study at 5 MHz, using a radiated power of 39 kw. Open circuit voltage was recorded at the receiver and the hourly median decibel values of voltage above one microvolt were obtained. The system loss excluding the ionospheric loss (Barghausen et al. 1969) was calculated and compared with an analysis of the 5 MHz data (Davis 1969) to obtain the measured monthly median midday absorption values. These absorption measurements are also plotted in figure 22 (solid curve). As can be seen, the agreement between the calculated absorption and the observed absorption appears to be satisfactory. Unfortunately, observations at 5

MHz were not available throughout the entire period of the experiment because of equipment difficulties.

As we have indicated in this paper, our formula was derived from vertical incidence data and then was generalized from theoretical considerations to the calculation of oblique data. In contrast to this approach, a formula derived from considerations of only oblique-incidence absorption data is given by Lucas and Haydon (1966),

$$L(\mathrm{dB})=\frac{677(1+0.0037R_{13})\,(\cos 0.881\chi)^{1.3}\sec\phi}{10.2+(f+f_H)^{1.98}}. \quad (22)$$

We have plotted as curve C in figure 22, for comparison purposes, the absorption values for the Long Branch–Boulder path as calculated by equation (22). As can be seen, this latter formula on this particular circuit does not agree with the observations as well as results calculated by equations (20) and (21). Other comparisons between observed and calculated signal strengths also indicate satisfactory agreement when equations (20) and (21) are used (Barghausen et al. 1969). The diurnal variation factor previously discussed has the solar zenith χ multiplied by the factor 0.893 to take into account layer sunrise and sunset times at 100 km. However, in the study indicated in figure 22, this factor was changed to 0.881 when the results of calculations by equations (20), (21), and (22) were compared.

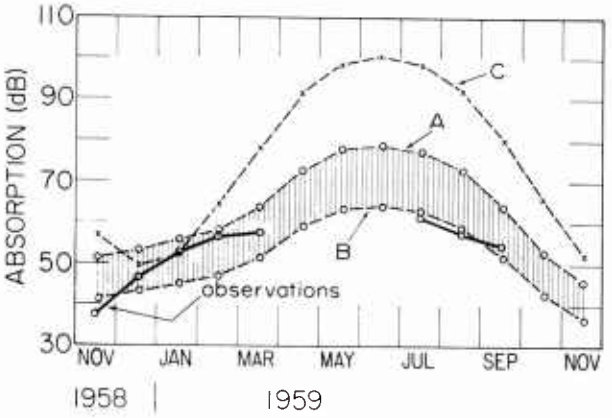

FIGURE 22.—Comparison of calculated and observed 5-MHz absorption on the Long Branch-Boulder path (1292 km).

Nighttime Absorption

Nighttime absorption at upper HF is not noticeable, but for oblique propagation at lower HF it amounts to a few decibels. A study of nighttime field strengths (Barghausen et al. 1969) indicated that the quantity

$$(1.0+0.0005R_{13})\cos^{N}\chi_{12}\left[\frac{\cos(0.893\chi)}{\cos(0.893\chi_{12})}\right]W$$

appearing in equation (20) (multiplied by the diurnal variation term discussed on page 5), when set to the value 0.01, gives calculated results in agreement with observations. In the above expression, χ_{12} represents the solar zenith angle at midday, and the factor 0.893 takes into account sunrise and sunset times at a height of 100 km above the earth.

CONCLUSION

The seasonal and solar cycle variation of ionospheric absorption is analyzed at each of the stations, Slough, Freiburg, Singapore, and Dakar. For the middle latitude stations, Slough and Freiburg, the analysis reconfirms the results of other published analyses, and, in addition, gives quantitatively the effects of the winter anomaly for the northern winter months. In the case of the equatorial stations, anomalous absorption is found to occur.

A comparison of the results of the four stations reveals the unexpected existence of a significant latitudinal variation of absorption not due to the $\cos^n\chi$ latitudinal variation (χ is the solar zenith angle; n is a constant for a given location). The latitudinal variation is of the same order of magnitude as the solar cycle variation of absorption.

The total variation of lower ionosphere absorption is separated into the four categories: (a) seasonal variation with latitudinal effects, (b) latitudinal variation, (c) solar cycle variation, and (d) winter anomaly effects. Empirically derived equations are given which permit the calculations of each of these four variations and also the calculation of the transmission losses of HF radio waves propagating via the ionosphere.

ACKNOWLEDGMENTS

The authors gratefully acknowledge the assistance they received from several persons. Valuable comments and suggestions were given by Thomas N. Gautier and Vaughn Agy of the Institute for Telecommunication Sciences, and Dr. Harold Leinbach of the Space Disturbances Laboratory, ESSA Research Laboratories in Boulder, Colorado. The personnel of the Aeronomy and Space Data Center of the Environmental Science Services Administration assisted in obtaining the published data.

REFERENCES

Appleton, E. V., "Regularities and Irregularities in the Ionosphere-I," *Proceedings of the Royal Society* (London), Series A: Mathematical and Physical Sciences, Vol. 162, October 1937, pp. 451–479.

Appleton, E. V., and Piggott, W. R., "Ionospheric Absorption Measurements During a Sunspot Cycle," *Journal of Atmospheric and Terrestrial Physics*, Vol. 5, No. 3, July 1954, pp. 141–172.

Barghausen, A. F., Finney, J. W., Proctor, L. L., and Schultz, L. D., "Predicting Long-Term Operational Parameters of High-Frequency Sky-Wave Telecommunication Systems," *ESSA Technical Report* ERL 110–ITS 78, ESSA Research Laboratories, Boulder, Colorado, May 1969, 290 pp.

Best, J. E., and Ratcliffe, J. A., "The Diurnal Variation of the Ionospheric Absorption of Wireless Waves," *Proceedings of the Physical Society* (London), Vol. 50, March 1938, pp. 233–246.

Bibl, K., Paul, A., and Rawer, K., "Die Frequenzabhängigkeit der ionosphärischen Absorption," (Frequency Dependence of Ionospheric Absorption), *Journal of Atmospheric and Terrestrial Physics*, Vol. 16, Nos. 3/4, November 1959, pp. 324–339.

Bibl, K., Paul, A., and Rawer, K., "Absorption in the D and E Regions and Its Time Variation," *Journal of Atmospheric and Terrestrial Physics*, Vol. 23, December 1961, pp. 244–259. [Also published as Chapter 22 in "Radio Wave Absorption in the Ionosphere," Proceedings, Advisory Group for Aeronautical Research and Development Committee, North Atlantic Treaty Organization, Fifth Meeting, Athens, Greece, Pergamon Press, New York, 379 pp.]

Bibl, K., and Rawer, K., "Contributions des regions D and E dans les mesures de l'absorption ionosphéric," (The Contribution of the D and E Regions in the Measurements of Ionospheric Absorption), *Journal of Atmospheric and Terrestrial Physics*, Vol. 2, No. 1, 1951, pp. 51–65.

Blair, J. C., Davis, R. M., Jr., and Kirby, R. C., "Frequency Dependence of D-Region Scattering at VHF," *Journal of Research*, National Bureau of Standards, Part D: Radio Propagation, Vol. 65, No. 5, September/October 1961, pp. 417–425.

Budden, K. G., *Radio Waves in the Ionosphere; the Mathematical Theory of the Reflection of Radio Waves from Stratified Ionized Layers*, Cambridge University Press (England), 1961, 542 pp.

Davies, K., and Hagg, E. L., "Ionospheric Absorption Measurements at Prince Rupert," *Journal of Atmospheric and Terrestrial Physics*, Vol. 6, No. 1, January 1955, pp. 18–32 (see p. 31).

Davis, R. M., Jr., private communication, 1969.

Delobeau, F., and Gallet, R., "L'amplitude anormale des effets saisonniers dans l'ionosphère équatoriale et la structure de la haute atmosphère," (Abnormal Amplitude of Seasonal Effects in the Equatorial Ionosphere and the Upper Atmospheric Structure), Académie des Sciences (Paris), *Comptes Rendus*, Vol. 239, No. 17, October 17, 1954, pp. 1067–1069.

Fejer, J. A., "The Absorption of Short Radio Waves in the Ionospheric D and E Regions," *Journal of Atmospheric and Terrestrial Physics*, Vol. 23, December 1961, pp. 260–274.

Harnischmacher, E., "L'influence solaire sur la couche E normal de l'ionosphère," (The Solar Influence on the Normal E Layer of the Ionosphere), Acadèmie des Science (Paris), *Comptes Rendus*, Vol. 230, 1950, pp. 1301–1302.

Hess, S. L., *Introduction to Theoretical Meteorology*, Henry Holt and Co., New York, 1959, 362 pp. (see Chapter 21).

Jackson, J. D., *Classical Electrodynamics*, J. Wiley and Sons, Inc., New York, N.Y., 1962, 641 pp.

Josephson, G. C., "An Improved Equation for Ionospheric Absorption," *Transactions on Antennas and Propagations*, Institute of Electrical and Electronic Engineers, Vol. 15, No. 2, March 1967, pp. 321–322.

Lucas, D. L., and Haydon, G. W., "Predicting Statistical Performance Indexes for High Frequency Ionospheric Telecommunications Systems," *ESSA Technical Report* IER 1-ITSA 1, ESSA Institutes for Environmental Research, Boulder, Colorado, August 1966, 167 pp.

Mitra, A. P., and Jain, V. C., "Interpretation of the Observed Zenith-Angle Dependence on Ionospheric Absorption," *Journal Geophysical Research*, Vol. 68, No. 9, May 1963, pp. 2367–2373.

Nicolet, M., and Bossy, L., "Sur l'absorption des ondes courtes dans l'ionosphère," (On the Absorption of Short Waves in the Ionosphere), *Annales de Géophysique*, Vol. 5, No. 4, October/December 1949, pp. 275–292.

Nicolet, M., "Composition et constitution de la haute atmosphere," (Composition and Structure of the Upper Atmosphere), *Geophysics, the Earths' Environment*, editor C. DeWitt, Gordon and Breach Publishing Company, New York, 1963, 258 pp.

Ostrow, S. M., and PoKempner, M., "The Differences in the Relationship Between Ionospheric Critical Frequencies and Sunspot Number for Different Sunspot Cycles," *Journal of Geophysical Research*, Vol. 57, No. 4, December 1952, pp. 473–480.

Panofsky, M. K. H., and Phillips, M., *Classical Electricity and Magnetism*, 2d edition, Addison-Wesley Publishing Company, Incorporated, New York, 1956, 494 pp.

Peebles, P. J. E., "Ionospheric Absorption Measurements on a Frequency of 2 MC/s at Baker Lake and Churchill," *Report PCC*, No. D48–95–11–02, Defense Research Telecommunications Establishment, Ottawa, Canada, 1956, 35 pp.

Piggott, W. R., "The Reflection and Absorption of Radio Waves in the Ionosphere," *Proceedings of the Institute of Electrical and Electronic Engineers*, Vol. 100, Part III, No. 64, March 1953, pp. 61–72.

Piggott, W. R., Beynon, W. J. G., Brown, G. M., and Little, C. G., "The Measurement of Ionospheric Absorption," *Annals of the International Geophysical Year*, Vol. III, Part II, 1957, pp. 177–203, Pergamon Press, London, New York, Paris, 381 pp.

Rao, M. K., Mazumdar, S. C., and Mitra, S. N., "Investigation of Ionospheric Absorption at Delhi," *Journal of Atmospheric and Terrestrial Physics*, Vol. 24, April 1962, pp. 245–256.

Ratcliffe, J. A., *The Magneto-Ionic Theory and Its Applications to the Ionosphere*, Cambridge University Press (England), 1962, 206 pp.

Rawer, K., "Les parametres de l'absorption des ondes par la couche D, et leur prévision," (The Absorption Parameters of Waves by the D Layer and Their Prediction), *Report SPIM* R 5 (Service de Prévision Ionosphérique Marine, Paris), January 1949, 20 pp.

Rawer, K., "Calculation of Sky-Wave Field Strength," *Wireless Engineer* (London), Vol. 29, No. 350, Nov. 1952, pp. 287–301.

Rawer, K., "Intercomparison of Different Calculation Methods of the Sky-Wave Field Strength," *Electromagnetic Wave Propagation*, editors M. Desirant and J. L. Michiels, Academic Press, New York, 1960a, pp. 647–659.

Rawer, K., "The Physical Interpretation of Absorption Measurements," *Some Ionospheric Results Obtained During the IGY*, edited by W. J. G. Beynon, URSI/AGI, Elsevier Publishing Company, Amsterdam and New York, 1960b, pp. 260–262.

Reed, R. J., "Wind and Temperature Oscillations in the Tropical Stratosphere," *Transactions of the American Geophysical Union*, Vol. 43, No. 1, March 1962, pp. 105–109.

Sen, H. K., and Wyller, A. A., "On the Generalization of the Appleton-Hartree Magnetoionic Formulas," *Journal of Geophysical Research*, Vol. 65, No. 12, December 1960, pp. 3931–3950.

Skinner, N. J., and Wright, R. W., "Absorption Measurements at Ibadan," (abstract) *URSI Symposium, Ionospheric Soundings in the IGY/IGC,* Nice (France), December 1961, p. 17.

Taylor, E. W., "Absorption of Radio Waves Reflected at Vertical Incidence as a Function of the Sun's Zenith Angle," *Journal of Research of the National Bureau of Standards,* Part D: Radio Propagation, Vol. 41, No. 6, December 1948, pp. 575–579.

Umlauft, G., "The Seasonal Variation of Daily Noon Absorption at Lindau/Harz and Tsumeb/SWA," (abstract) *URSI Symposium Ionospheric Soundings in the IGY/IGC,* Nice (France), December 1961, p. 20.

Whitehead, J. D., "The Distance Attenuation of Radio Waves Reflected at Vertical Incidence From the Ionosphere," *Journal of Atmospheric and Terrestrial Physics,* Vol. 12, No. 2/3, 1958, pp. 150–152.

Appendix

Absorption Data Sources

This section gives the sources of the published original absorption data obtained by the reflection method. For the convenience of future studies, and in view of the difficulty of obtaining the absorption material which was dispersed in a large number of different bulletins, it is believed valuable to assemble in homogeneous form all the monthly median A-values from the beginning of the series—January 1935 until the last published value, June 1962. The sources of this data are given in the table.

Absorption data sources

Station	Period	Publication
Slough	Jan. 1935–June 1953	Monthly Bulletin of Ionosphere Characteristics, B-Series, Slough, England
Freiburg	Dec. 1948–Mar. 1951	Observations Ionosphériques, SPIM–O Series
	Jan. 1952–Dec. 1955	Observations de l'Absorption Ionosphérique, SPIM–R16
	Jan. 1956–June 1962	Ionosphären Daten, Absorptions Messungen, Nr. 1 through Nr. 7
Singapore	Sept. 1949–June 1953	Monthly Bulletin of Ionosphere Characteristics, B–Series, Slough, England
	July 1953–Apr. 1954	Private Information
Dakar	May 1951–Dec. 1955	Observations de l'Absorption Ionosphérique, SPIM–R16

With the exception of part of the Singapore data, all of the data listed in the above table and used in this report was made available to the present authors through the facilities of the Aeronomy and Space Data Center of the Environmental Science Services Administration in Boulder, Colorado.

Description of Tables

The appendix contains four tables, one table for each of the ionosphere stations, Slough, Freiburg, Dakar, and Singapore. Each table contains the following:

1. The published absorption index A-values from the sources given in the preceding table.
2. The smoothed absorption index A_{13}-values.
3. The ratio $I=A/A_{13}$ for each month for which data were available.
4. The average I-values for each month, designated $\bar{I}$. These values are also given in table 2 of the text.

TABLE A–I. — *Slough*

YEAR

A - VALUES

	1935	1936	1937	1938	1939	1940	1941	1942	1943	1944	
JAN.	194	294	400	380	410	376	824	342	298	356	JAN.
FEB.	364	378	434	376	340	484	388	322	234	294	FEB.
MAR.	370	282	470	364	446	430	384	380	348	356	MAR.
APR.	446	438	1022	540	658	512	408	492	416	550	APR.
MAY	610	868	826	564	634	598	388	388	458	526	MAY
JUNE	594	636	934	534	564	638	496	382	436	544	JUNE
JULY	576	564	728	740	676	634	524	366	484	526	JULY
AUG.	428	446	650	702	638	572	438	376	458	496	AUG.
SEPT.	392	498	516	462	540	408	446	364	490	438	SEPT.
OCT.	340	356	516	340	532	354	280	296	306	352	OCT.
NOV.	276	290	378	300	288	294	252	340	312	234	NOV.
DEC.	222	446	488	388	344	[550]	290	348	356	316	DEC.

A_{13} - VALUES

JAN.		436	574	516	504	516	428	378	366	426	JAN.
FEB.		426	580	514	496	508	412	366	372	426	FEB.
MAR.		430	586	500	484	490	402	360	382	426	MAR.
APR.		430	582	486	490	476	392	348	376	414	APR.
MAY		428	582	474	486	458	384	354	378	410	MAY
JUNE		442	596	476	488	462	384	362	378	410	JUNE
JULY	388	456	592	470	488	462	384	362	380	406	JULY
AUG.	402	466	590	466	494	464	382	354	378	400	AUG.
SEPT.	396	474	584	462	500	456	382	356	388	402	SEPT.
OCT.	400	530	590	486	514	454	390	358	404	402	OCT.
NOV.	432	562	554	494	510	444	388	354	412	398	NOV.
DEC.	438	566	530	494	510	436	388	358	420	378	DEC.

I - VALUES

JAN.		0.674	0.697	0.736	0.813	0.729	1.925	0.905	0.814	0.836	JAN.
FEB.		0.887	0.748	0.732	0.685	0.953	0.942	0.880	0.629	0.690	FEB.
MAR.		0.656	0.802	0.728	0.921	0.878	0.955	1.056	0.911	0.836	MAR.
APR.		1.019	1.756	1.111	1.343	1.076	1.041	1.414	1.106	1.328	APR.
MAY		2.028	1.419	1.190	1.305	1.306	1.010	1.096	1.212	1.283	MAY
JUNE		1.439	1.567	1.122	1.156	1.381	1.292	1.055	1.153	1.327	JUNE
JULY	1.484	1.237	1.230	1.574	1.385	1.372	1.365	1.011	1.274	1.296	JULY
AUG.	1.065	0.957	1.102	1.506	1.291	1.233	1.147	1.062	1.212	1.240	AUG.
SEPT.	0.990	1.051	0.884	1.000	1.080	0.895	1.168	1.022	1.263	1.090	SEPT.
OCT.	0.850	0.672	0.875	0.700	1.035	0.780	0.718	0.827	0.757	0.876	OCT.
NOV.	0.639	0.516	0.682	0.607	0.565	0.662	0.649	0.960	0.757	0.588	NOV.
DEC.	0.507	0.788	0.921	0.785	0.674	[1.261]	0.747	0.972	0.848	0.836	DEC.

[ ]: means data were missing and for purposes of continuity have been interpolated by the authors.

TABLE A–I. – *Slough* – Continued

YEAR

	1945	1946	1947	1948	1949	1950	1951	1952	1953

A - VALUES

JAN.	410	410	440	540	550	365	460	645	505
FEB.	280	440	490	400	440	470	480	490	360
MAR.	320	420	510	440	410	390	310	350	395
APR.	360	420	460	530	455	440	465	370	430
MAY	370	440	580	560	435	440	500	410	400
JUNE	390	480	570	480	440	415	520	425	420
JULY	370	510	550	520	470	420	520	415	
AUG.	360	510	590	520	490	460	515	440	
SEPT.	350	460	560	445	415	480	480	390	
OCT.	330	350	400	385	410	400	340	355	
NOV.	310	360	350	380	390	415	410	340	
DEC.	370	360	390	460	410	530	495	330	

A_{13} - VALUES

JAN.	364	400	472	485	455	425	458	451	
FEB.	354	412	480	483	452	424	466	445	
MAR.	342	420	482	472	444	423	467	435	
APR.	334	420	479	458	442	422	457	426	
MAY	330	422	479	457	442	423	457	426	
JUNE	342	426	480	465	444	433	463	420	
JULY	348	430	494	478	437	437	472	420	
AUG.	358	436	492	470	431	446	475	398	
SEPT.	370	442	488	471	427	434	465	391	
OCT.	376	446	490	472	429	440	469	397	
NOV.	382	458	496	465	428	444	465	400	
DEC.	392	468	489	455	427	450	459	400	

I - VALUES

JAN.	1.126	1.025	0.932	1.134	1.209	0.859	1.004	1.430
FEB.	0.791	1.068	1.021	0.828	0.973	1.108	1.030	1.101
MAR.	0.936	1.000	1.058	0.932	0.923	0.922	0.664	0.805
APR.	1.078	1.000	0.960	1.157	1.029	1.043	1.018	0.869
MAY	1.121	1.043	1.211	1.225	0.984	1.040	1.094	0.962
JUNE	1.140	1.127	1.188	1.032	0.991	0.958	1.123	1.012
JULY	1.063	1.186	1.113	1.088	1.076	0.961	1.102	0.988
AUG.	1.006	1.170	1.199	1.106	1.137	1.031	1.084	1.106
SEPT.	0.946	1.041	1.148	0.945	0.972	1.106	1.032	0.997
OCT.	0.878	0.785	0.816	0.816	0.956	0.909	0.725	0.894
NOV.	0.812	0.786	0.706	0.817	0.911	0.935	0.882	0.850
DEC.	0.944	0.769	0.798	1.011	0.960	1.178	1.078	0.825

$\bar{I}$ - VALUES

JAN.	0.990
FEB.	0.886
MAR.	0.881
APR.	1.138
MAY	1.208
JUNE	1.180
JULY	1.211
AUG.	1.147
SEPT.	1.035
OCT.	0.826
NOV.	0.740
DEC.	0.884

TABLE A–II. — *Freiburg*

A - VALUES

	1948	1949	1950	1951	1952	1953	1954	1955	1956	1957	
JAN.		428	331	280	380	280	290	190	430	410	JAN.
FEB.		360	485	390	390	260	250	250	390	420	FEB.
MAR.		380	336	250	410	260	280	280	400	420	MAR.
APR.		395	450		380	270	280	380	470	600	APR.
MAY		450	500		400	340	410	360	420	600	MAY
JUNE		492	450		410	310	320	280	570	690	JUNE
JULY		552	480		470	300	320	270	640	660	JULY
AUG.		519	570		440	300	310	440	400	540	AUG.
SEPT.		481	431		400	280	300	340	520	650	SEPT.
OCT.		322	280		260	200	310	360	490	540	OCT.
NOV.	330	336	360		200	240	300	360	470	510	NOV.
DEC.	365	361	370		290	200	310	400	410	670	DEC.

A_{13} - VALUES

JAN.			467	[425]	[388]	314	282	297	422	518	JAN.
FEB.			468	[422]	[387]	301	283	306	432	510	FEB.
MAR.			461	[421]	[379]	288	283	308	438	529	MAR.
APR.			444	[421]	[371]	273	285	312	450	531	APR.
MAY		451	447	[420]	[369]	271	293	317	458	532	MAY
JUNE		453	450	[419]	[367]	271	298	324	462	548	JUNE
JULY		451	444	[418]	365	271	298	333	463	566	JULY
AUG.		455	444	[413]	356	269	294	349	462	589	AUG.
SEPT.		453	429	[409]	346	271	297	361	464	609	SEPT.
OCT.		459	[428]	[406]	335	272	304	375	480	634	OCT.
NOV.		468	[426]	[398]	332	283	310	378	490	636	NOV.
DEC.		468	[426]	[390]	322	281	301	395	510	651	DEC.

I - VALUES

JAN.			0.709	[0.659]	[0.980]	0.892	1.028	0.640	1.019	0.791	JAN.
FEB.			1.036	[0.924]	[1.008]	0.864	0.883	0.817	0.903	0.824	FEB.
MAR.			0.729	[0.594]	[1.082]	0.903	0.989	0.909	0.913	0.794	MAR.
APR.			1.014		[1.024]	0.989	0.982	1.218	1.044	1.130	APR.
MAY		0.998	1.119		[1.186]	1.255	1.399	1.136	0.917	1.128	MAY
JUNE		1.086	1.000		[1.117]	1.144	1.074	0.864	1.234	1.259	JUNE
JULY		1.224	1.081		1.288	1.107	1.074	0.811	1.382	1.166	JULY
AUG.		1.141	1.284		1.236	1.115	1.054	1.261	0.866	0.917	AUG.
SEPT.		1.062	1.005		1.156	1.033	1.010	0.942	1.121	1.067	SEPT.
OCT.		0.702	[0.654]		0.776	0.735	1.020	0.960	1.021	0.852	OCT.
NOV.		0.718	[0.845]		0.602	0.848	0.968	0.952	0.959	0.802	NOV.
DEC.		0.771	[0.868]		0.901	0.712	1.030	1.013	0.804	1.029	DEC.

TABLE A–II. — *Freiburg* — Continued

YEAR

	1958	1959	1960	1961	1962

A - VALUES

JAN.	660	720	530	420	380
FEB.	690	600	470	400	273
MAR.	680	610	520	390	315
APR.	740	770	650	510	499
MAY	640	740	640	580	502
JUNE	800	730	680	600	512
JULY	820	750	650	670	
AUG.	700	600	660	520	
SEPT.	740	660	570	470	
OCT.	600	510	400	380	
NOV.	390	440	440	370	
DEC.	510	490	480	270	

A_{13} - VALUES

JAN.	662	668	584	521	
FEB.	664	651	577	511	
MAR.	680	647	574	496	
APR.	676	630	555	482	
MAY	664	617	541	479	
JUNE	664	626	545	466	
JULY	668	627	539	458	
AUG.	663	608	537	447	
SEPT.	657	602	531	441	
OCT.	664	604	530	449	
NOV.	664	594	524	448	
DEC.	672	590	522	443	

I - VALUES

JAN.	0.997	1.078	0.908	0.806	
FEB.	1.039	0.922	0.815	0.783	
MAR.	1.000	0.943	0.906	0.809	
APR.	1.095	1.222	1.171	1.058	
MAY	0.964	1.199	1.183	1.211	
JUNE	1.205	1.166	1.248	1.288	
JULY	1.228	1.196	1.206		
AUG.	1.056	0.987	1.229		
SEPT.	1.126	1.096	1.073		
OCT.	0.904	0.844	0.755		
NOV.	0.587	0.740	0.840		
DEC.	0.759	0.830	0.920		

$\bar{I}$ - VALUES

JAN.	0.876
FEB.	0.901
MAR.	0.881
APR.	1.086
MAY	1.142
JUNE	1.140
JULY	1.160
AUG.	1.104
SEPT.	1.063
OCT.	0.838
NOV.	0.806
DEC.	0.876

TABLE A–III. — *Dakar*

YEAR

	1951	1952	1953	1954	1955

A - VALUES

JAN.		310	220	210	140
FEB.		140	170	260	170
MAR.		120	310	290	170
APR.		400	440	330	190
MAY	370	462	350	450	170
JUNE	450	210	100	310	200
JULY	310	190	360	350	180
AUG.	340	120	330	350	210
SEPT.	180	440	390	270	310
OCT.	180	480	370	200	380
NOV.	210	280	230	230	330
DEC.	270	210	210	260	220

A_{13} - VALUES

JAN.		256	282	315	222
FEB.		241	293	314	211
MAR.		249	314	309	208
APR.		272	308	295	216
MAY		279	289	284	226
JUNE		279	284	286	225
JULY		276	284	281	
AUG.		265	287	278	
SEPT.		278	296	271	
OCT.		302	298	263	
NOV.	288	299	298	251	
DEC.	276	271	295	232	

I - VALUES

JAN.		1.211	.780	.667	.631
FEB.		.581	.580	.828	.806
MAR.		.482	.987	.939	.817
APR.		1.471	1.429	1.119	.880
MAY		1.656	1.311	1.585	.752
JUNE		.753	.352	1.084	.889
JULY		.688	1.268	1.246	
AUG.		.453	1.150	1.259	
SEPT.		1.583	1.318	.996	
OCT.		1.589	1.242	.760	
NOV.	.729	.936	.772	.916	
DEC.	.978	.775	.712	1.121	

$\bar{I}$ - VALUES

JAN.	.822
FEB.	.699
MAR.	.806
APR.	1.225
MAY	1.326
JUNE	.770
JULY	1.067
AUG.	.954
SEPT.	1.299
OCT.	1.197
NOV.	.838
DEC.	.896

TABLE A–IV.—*Singapore*

YEAR

	1949	1950	1951	1952	1953	1954

A - VALUES

JAN.		380	[330]	315	320	280
FEB.		405	[360]	315	330	305
MAR.		470	390	320	370	320
APR.		520	405	330	350	270
MAY		500	[375]	310	300	
JUNE		325	350	[305]	270	
JULY		330	310	300	270	
AUG.		400	360	340	305	
SEPT.	515	380	400	380	350	
OCT.	545	375	425	400	365	
NOV.	505	350	380	360	295	
DEC.	410	300	310	330	[287]	

A_{13} - VALUES

JAN.			358	337	332	
FEB.			360	339	333	
MAR.		437	360	341	333	
APR.		426	364	341	332	
MAY		412	364	336	324	
JUNE		396	361	332	319	
JULY		390	362	333	315	
AUG.		388	361	334	314	
SEPT.		387	358	338	313	
OCT.		382	353	340	305	
NOV.		371	346	338		
DEC.		359	341	335		

I - VALUES

JAN.			.922	.935	.964	
FEB.			1.000	.929	.991	
MAR.		1.076	1.083	.938	1.111	
APR.		1.221	1.113	.968	1.054	
MAY		1.214	1.030	.923	.926	
JUNE		.821	.970	.919	.846	
JULY		.846	.856	.901	.857	
AUG.		1.031	.997	1.018	.971	
SEPT.		.982	1.117	1.124	1.118	
OCT.		.982	1.204	1.176	1.197	
NOV.		.943	1.098	1.065		
DEC.		.836	.909	.985		

$\bar{I}$ - VALUES

JAN.	.940
FEB.	.973
MAR.	1.052
APR.	1.089
MAY	1.023
JUNE	.889
JULY	.865
AUG.	1.004
SEPT.	1.085
OCT.	1.140
NOV.	1.035
DEC.	.910

U.S. GOVERNMENT PRINTING OFFICE : 1970 OL—387–150